



1 **Towards a Dynamic Earthquake Risk Framework for** 2 **Switzerland**

3
4 Maren Böse^{1*}, Laurentiu Danciu¹, Athanasios Papadopoulos¹, John Clinton¹, Carlo Cauzzi¹,
5 Irina Dallo¹, Leila Mizrahi¹, Tobias Diehl¹, Paolo Bergamo¹, Yves Reuland², Andreas
6 Fichtner³, Philippe Roth¹, Florian Haslinger¹, Frederick Massin¹, Nadja Valenzuela¹, Nikola
7 Blagojević², Lukas Bodenmann², Eleni Chatzi², Donat Fäh¹, Franziska Glueer¹, Marta Han¹,
8 Lukas Heiniger¹, Paulina Janusz¹, Dario Jozinovic¹, Philipp Kästli¹, Federica Lanza¹, Timothy
9 Lee¹, Panagiotis Martakis², Michèle Marti¹, Men-Andrin Meier⁴, Banu Mena Cabrera¹, Maria
10 Mesimeri¹, Anne Obermann¹, Pilar Sanchez-Pastor¹, Luca Scarabello¹, Nicolas Schmid¹,
11 Anastasiia Shynkarenko¹, Bozidar Stojadinovic², Domenico Giardini⁴, and Stefan Wiemer¹

12
13
14 ¹ Swiss Seismological Service (SED) at ETH Zurich, Sonneggstrasse 5, 8092 Zurich, 8092, Switzerland

15 ² Institute of Structural Engineering (IBK) at ETH Zurich, Stefano-Frascini-Platz 5, 8093 Zurich, Switzerland

16 ³ Seismology and Wave Physics (SWP) at ETH Zurich, Sonneggstrasse 5, 8092 Zurich, 8092, Switzerland

17 ⁴ Seismology and Geodynamics (SEG) at ETH Zurich, Sonneggstrasse 5, 8092 Zurich, 8092, Switzerland

18

19

20 *Correspondence to: Maren Böse (maren.boese@sed.ethz.ch)

21 **Abstract.** Scientists at ETH Zurich from different disciplines are developing a dynamic, harmonised and user-
22 centred earthquake risk framework for Switzerland, relying on a continuously evolving earthquake catalogue
23 generated by the SED using the national seismic networks. This framework uses all available information to assess
24 seismic risk at various stages and facilitates widespread dissemination and communication of the resulting
25 information. Earthquake risk products and services include Operational Earthquake (Loss) Forecasting (OE[L]F),
26 Earthquake Early Warning (EEW), ShakeMaps, Rapid Impact Assessment (RIA), Structural Health Monitoring
27 (SHM), as well as Recovery and Rebuilding Efforts (RRE). Standardisation of products and workflows across
28 various applications is essential for achieving broad adoption, universal recognition, and maximum synergies. In
29 the Swiss dynamic earthquake risk framework, the harmonisation of products into seamless solutions that access
30 the same databases, workflows, and software is a crucial component to ensure standardisation. A user-centred
31 approach utilising quantitative and qualitative social science tools like online surveys and focus groups is a
32 significant innovation featured in all products and services. Here we report on the key considerations and
33 developments of the framework and its components.

34 **Short Summary.** We are developing an interdisciplinary dynamic earthquake risk framework for Switzerland for
35 advancing earthquake risk mitigation. It includes various earthquake risk products and services, such as
36 Operational Earthquake Forecasting and Earthquake Early Warning, and adopts a user-centred approach.
37 Standardisation is crucial for widespread adoption and recognition, and the harmonisation of products into
38 seamless solutions that access the same databases, workflows, and software is a crucial component.

39 **Keywords:** seismic hazard, seismic risk, seismic network, earthquake forecasting, earthquake early warning,
40 rapid loss assessment, structural health monitoring, recovery and rebuilding efforts, earthquake communication

41



42 1. Introduction

43 Europe faces a significant earthquake risk due to its tectonic situation, high population density, business value,
44 and the age and condition of buildings (e.g., Danciu *et al.*, 2022; Crowley *et al.*, 2022). This includes areas with
45 moderate seismic activity, such as Switzerland, where earthquakes have the potential to cause significant loss,
46 with projected costs of major events exceeding Euro 100 billion (Wiemer *et al.*, 2016; Wiemer *et al.*, 2023).
47 Building codes and retrofitting are the most effective measures to reduce earthquake risk, but emerging
48 technologies, such as Operational Earthquake Forecasting (OEF) or Earthquake Early Warning (EEW), can also
49 improve resilience by means of reducing exposure (e.g., Cauzzi *et al.*, 2016; Papadopoulos *et al.*, 2023).

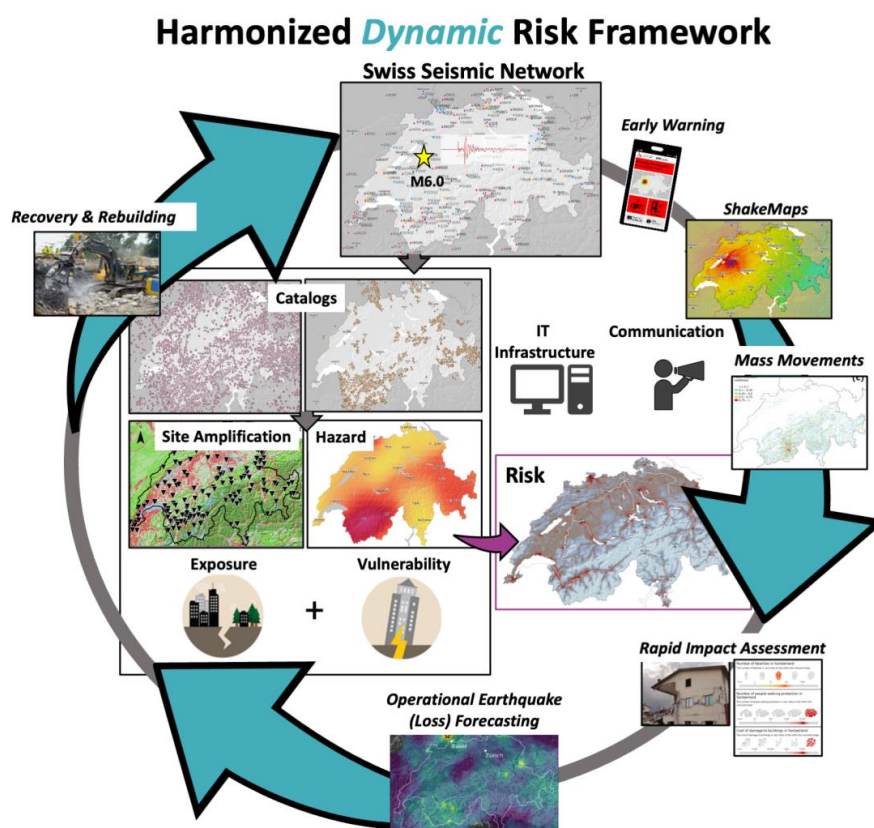
50 The national Seismic Hazard Model (SUIhaz2015; Wiemer *et al.*, 2016) and the recently released first national
51 Earthquake Risk Model of Switzerland (ERM-CH23; Wiemer *et al.*, 2023; Papadopoulos *et al.*, *subm.*) serve as
52 the basis for tools and systems being developed as part of a dynamic, harmonised and user-centred earthquake
53 risk framework for Switzerland. This framework uses all available information to assess seismic risk at various
54 stages of the earthquake cycle (**Figure 1**), and facilitates widespread dissemination and communication of the
55 resulting information. This involves various services, products, and research developed at the Swiss Seismological
56 Service (SED), the Department of Earth Science, and the Institute of Structural Engineering (IBK) at the
57 Eidgenössische Technische Hochschule (ETH) Zurich, including Operational Earthquake (Loss) Forecasting
58 (OE[L]F), Earthquake Early Warning (EEW), ShakeMaps, Rapid Impact Assessment (RIA), Structural Health
59 Monitoring (SHM), as well as Recovery and Rebuilding Efforts (RRE).

60 The harmonisation of products and workflows across various applications is crucial for broad adoption and
61 universal recognition of products, as well as to maximise synergies and impact. A crucial component of the Swiss
62 dynamic risk framework is, therefore, the standardisation into seamless products that access the same databases,
63 workflows, and software, and are based on standard models. For instance, the current RIA for Switzerland utilises
64 Swiss ShakeMap (Cauzzi *et al.*, 2015; 2022), which provides ground-motion maps in near real-time and employs
65 the same site amplification layers (Bergamo *et al.*, 2023) used in ERM-CH23. Rapid impact is calculated using
66 OpenQuake (Pagani *et al.*, 2014) for scenario products, RIA, and probabilistic products, while the impact on
67 people and buildings is determined from national building databases and their vulnerability. OELF calculations
68 employ short-term seismicity forecasts in synergy with components of the hazard and risk models utilised for
69 long-term hazard and risk calculations and RIA products. All products are informed by a single, continuously
70 evolving earthquake catalogue as well as continuous waveforms generated by the SED using the national seismic
71 networks.

72 All products and services feature a significant innovation, namely a user-centred approach that utilises quantitative
73 and qualitative social science tools such as online surveys and focus groups. The visual representation of rapid
74 impact, for instance, was created based on feedback from focus groups and discussions with stakeholders at the
75 federal and cantonal levels, featuring new visualisations of uncertainties. The risk map was adjusted to the public
76 needs which were assessed with a representative, nationwide survey.



77 Here we report on the key components of the Swiss dynamic, harmonised and user-centred earthquake risk
 78 framework which were mostly developed within the scope of the European Union Horizon 2020 *Real-time*
 79 *earthquake risk reduction for a Resilient Europe* (RISE)¹ project (**Figure 1**). We start with a summary of the
 80 seismic hazard and risk in Switzerland and then continue with a description of the recent advancements in seismic
 81 monitoring capabilities over the last decade, which are crucial for downstream risk mitigation products and
 82 services, on which we focus in the second part of this paper. Finally, we discuss the SED strategy for
 83 implementation and communication of earthquake hazard and risk products with the public and stakeholders in
 84 Switzerland.



85

86 **Figure 1:** Schematic representation of the dynamic risk concept.

87

88 1.1 Seismic Hazard and Risk in Switzerland

89 Switzerland is exposed to a considerable threat of earthquakes. Around 1000 to 1500 earthquakes are detected in
 90 Switzerland and its neighbouring countries every year, including 20 to 30 events that the population feels (**Figure**

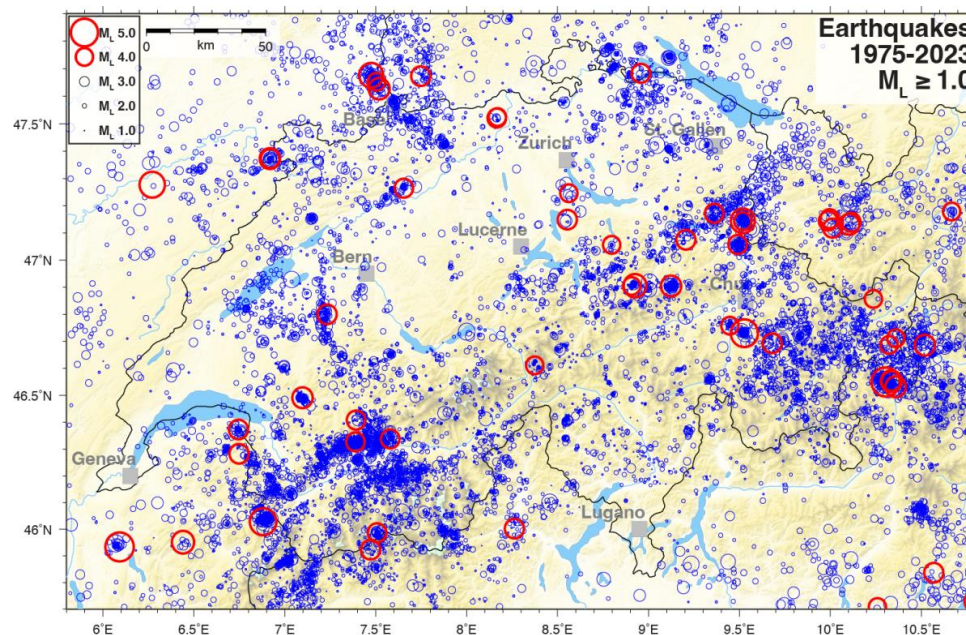
¹ <http://www.rise-eu.org/home/> last accessed July 2023



91 2). SUIhaz2015 (**Figure 3a**; Wiemer *et al.*, 2016), which assesses the likelihood of ground shaking, forecasts that
92 earthquakes of magnitude $M \geq 5$ are likely to occur every 8 to 15 years. The severity of impacts on buildings
93 depends on the location and depth of the earthquake. Earthquakes with a magnitude of 6 or greater, which can
94 cause extensive and severe damage, occur on average every 50 to 150 years and can strike any part of Switzerland
95 at any time. The last earthquake of this magnitude occurred close to the town of Sierre in the Upper Valais in 1946
96 (Fäh *et al.*, 2011). The canton of Valais faces the highest level of seismic hazard in Switzerland, followed by
97 Basel, Grisons, the St. Gallen Rhine Valley, and Central Switzerland.

98 The seismic hazard model SUIHAZ2015 has been implemented in the most recent version of Swiss building code
99 SIA 261 (2020). The 2015 Swiss seismic hazard model updated the hazard model from 2003 (Giardini *et al.*,
100 2004). The first seismic hazard model for Switzerland used in Swiss building codes until 2003 was the one of
101 Sägesser and Mayer-Rosa (1978) which was based on the historical catalogue available at the time and on
102 macroseismic intensity.

103



104
105
106

Figure 2: Map of Switzerland and the surrounding area showing all seismicity with $ML \geq 1.0$ since 1975 in the SED earthquake catalogue (bulletin locations). Events with $ML \geq 4.0$ are highlighted by bold red circles.

107 Methods for estimating site-specific amplification and local seismic hazard were developed at SED during the
108 past decades and were implemented in microzonation studies, e.g., as for the region of Basel (e.g., Fäh and
109 Huggenberger, 2006). A number of approaches were developed to estimate site-specific amplification based on
110 geophysical measurements and earthquake recordings (e.g., Edwards *et al.*, 2013; Michel *et al.*, 2017; Poggi *et al.*,
111 2017; Perron *et al.*, 2022; Panzera *et al.*, 2021, 2022). Recently, a project started to update the microzonation

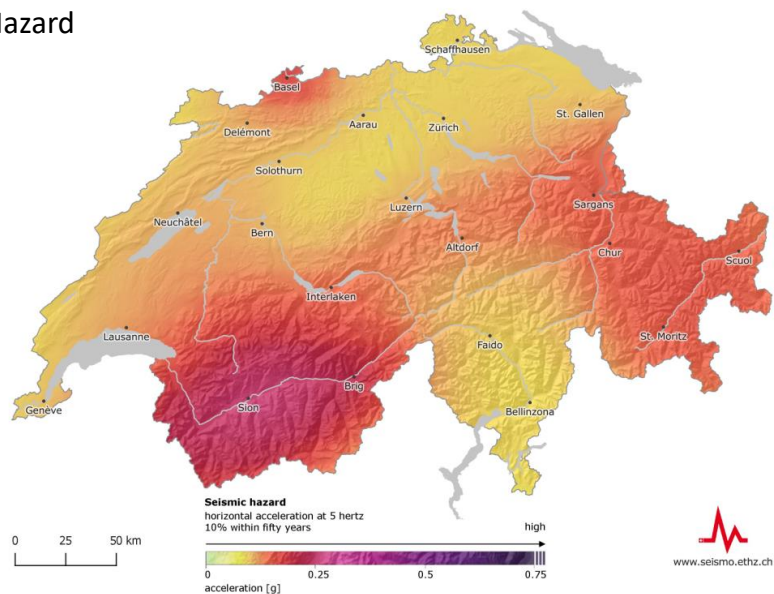


112 for the Basel region. All this experience was used to define the elastic response spectra in the Swiss building code
113 (2020) and to implement a national regulation related to microzonation in SIA 261/1 (2020).

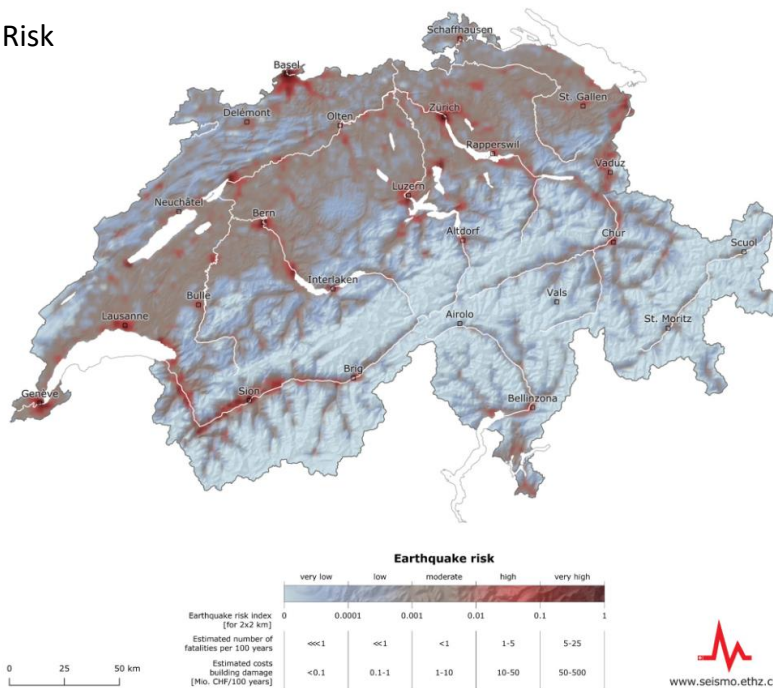
114 Geographic features, such as large and deep peri-alpine lakes, steep slopes, and alluvial basins with a high-water
115 table, make Switzerland susceptible to secondary hazards (e.g., Fritsche *et al.*, 2012; Fäh *et al.*, 2012). Using
116 geophysical imaging, seismic monitoring, numerical modelling and other techniques, the SED has been
117 conducting research on earthquake-induced hazards, including (i) rockfalls and landslides (e.g., Burjanek *et al.*,
118 2018; Kleinbrod *et al.*, 2018; Glueer *et al.*, 2021; Häusler *et al.*, 2022); (ii) lake tsunamis (e.g., Strupler *et al.*,
119 2018; Kremer *et al.*, 2022; Shynkarenko *et al.*, 2022); and (iii) liquefaction (e.g., Fritsche *et al.*, 2012; Roten *et al.*,
120 2014; Janusz *et al.*, 2022). Findings from these studies have been incorporated into rapid estimates of
121 earthquake-induced mass movements and liquefaction probabilities in Switzerland via the SED ShakeMap
122 application (Cauzzi *et al.*, 2018a; Section 3.3).



(a) Hazard



(b) Risk



123
 124
 125
 126
 127
 128
 129

Figure 3: (a) Swiss Hazard Map (SUIhaz2015; @Swiss Seismological Service) showing the horizontal acceleration at 5 Hz; the probability of a building constructed on rocky subsoil experiencing this is 10% within 50 years (i.e., mean return period of 475 years). On average, 5 Hz represents the natural frequency of buildings with two to five floors, which make up the largest proportion of construction in Switzerland. 475 years is the value that underlies the Swiss Seismic Building Codes: an earthquake-resistant residential or office building should be able to withstand an earthquake that occurs where the building is situated within 475 years on average. (b) National Earthquake Risk Model



130 of Switzerland (ERM-CH23; @Swiss Seismological Service). The color scale refers to a composite index based on
131 average annual structural/nonstructural loss and fatalities.

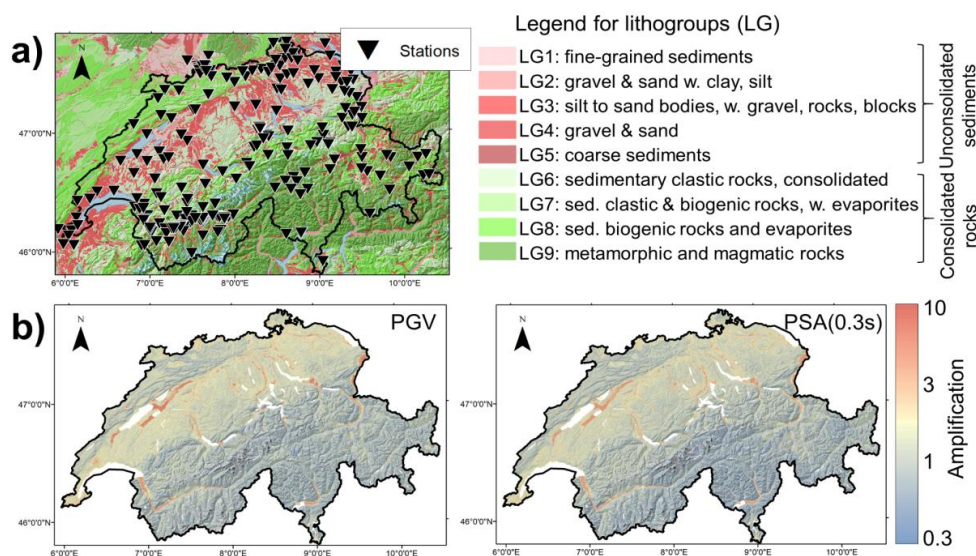
132

133 While seismic hazard in Switzerland has been extensively studied, a formal effort to quantify seismic risk, which
134 assesses the potential impact of earthquakes on both people and structures, as well as the resulting financial losses,
135 was not available in the public domain until recently. In March 2023, the SED in partnership with the Federal
136 Office for the Environment (FOEN) and the Federal Office for Civil Protection (FOCP) released the first National
137 Earthquake Risk Model of Switzerland (ERM-CH23; **Figure 3b**; Wiemer *et al.*, 2023). ERM-CH23 is
138 implemented for use with OpenQuake (Pagani *et al.*, 2014), developed by the Global Earthquake Model (GEM)
139 foundation. As with most contemporary risk models, ERM-CH23 follows a modular structure (Mitchell-Wallace
140 *et al.*, 2017), with five generally decoupled components pertaining to seismic hazard on a reference rock,
141 amplification, structural vulnerability, exposure, and consequence models. These components were developed
142 through collaboration with national and international partners. Unlike past attempts that sought to assess
143 earthquake risk at a continental (Crowley *et al.*, 2021) or global scale (Silva *et al.*, 2020), ERM-CH23 is largely
144 supported by high-quality local data, including a database of more than 2 million building objects that was
145 compiled by the FOEN. Together with ground surveys to assess the frequency of different building materials,
146 conducted by partners at the École Polytechnique Fédérale de Lausanne (EPFL), they underpin the ERM-CH23
147 exposure model.

148

149 ERM-CH23 has been developed to estimate the economic damage in Switzerland caused by earthquakes, which
150 resulted in a projected average cost of CHF 11 to 44 billion for building and contents alone, over a 100-year
151 period. Urban areas, particularly the cities of Basel, Geneva, Zurich, Lucerne, and Bern, face the greatest risk due
152 to their size and the concentration of people and assets that could be impacted by an earthquake. Additionally,
153 these cities contain numerous vulnerable buildings located on soft soil types, which can significantly amplify
154 seismic waves. As a culmination of many years of research and expertise within the SED (e.g., Michel *et al.*,
155 2017, Hobiger *et al.*, 2021, Bergamo *et al.*, 2021), a national site amplification model (**Figure 4**) has been created
156 as part of ERM-CH23, using geo-spatial prediction techniques constrained on local site response measured at
157 instrumented sites (Bergamo *et al.*, 2023). This model is based on (i) the direct mapping of observed site
158 amplification factors at about 245 seismic stations, extracted with empirical spectral modelling technique (ESM,
159 Edwards *et al.*, 2013); and (ii) layers of site condition indicators (multi-scale topographic slope, estimated bedrock
160 depth, lithological classification of soil; **Figure 4a**). The dataset of empirical amplification factors was finally
161 interpolated over the national territory using site condition proxies as predictor variables and the regression kriging
162 algorithm (Hengl *et al.*, 2007) as a geo-spatial prediction framework. The resulting amplification model consists
163 of four soil response layers for PGV, PSA(1.0s), PSA(0.6s) and PSA(0.3s) (e.g., **Figure 4b**), each with associated
164 maps of epistemic (ϕ_{S2S}) and aleatory (ϕ_{S2S}) variability following the definition in Al Atik *et al.* (2010). The
165 amplification maps for PGV, PSA(1.0s) and PSA(0.3s) were also converted into layers of aggravation or reduction
166 of macroseismic intensity by means of the relations of Faenza & Michelini (2010, 2011).

167



168

169 **Figure 4:** (a) Geographical locations of the 243 (urban) free-field stations having recorded at least 5 earthquakes with
 170 signal-to-noise ratios > 3 in the period 2000 – 2021, superimposed on the lithological classification of Switzerland
 171 employed to derive the national soil response model. (b) PGV (left) and PSA(0.3s) (right) amplification maps (referred
 172 to $V_{s30} = 1105$ m/s), part of the national soil response model (Bergamo *et al.*, 2023).

173 **2. Seismic Monitoring**

174 **2.1 Swiss Seismic Network**

175

176 The Swiss Seismic Network counts today about 220 permanent stations (network code CH; Swiss Seismological
 177 Service at ETH Zurich, 1983) with the aim to monitor the seismic activity in Switzerland, support scientific
 178 research, and assess seismic risk (Clinton *et al.*, 2011; Diehl *et al.*, 2021b; **Figure 5**). The network is divided into
 179 two main groups of stations. The first group is composed of about 50 backbone broadband stations (known as the
 180 ‘SDSNet’) that have very sensitive seismic sensors (velocity instruments, often referred to as “weak-motion”)
 181 placed in quiet areas with optimal vault conditions. These stations are evenly spread throughout Switzerland and
 182 can detect and locate microseismic activity. Each of these sites also has a state-of-the-art force-balance
 183 accelerometer (often referred to as “strong-motion” instrument). The second group is composed of approximately
 184 150 strong-motion stations (known as ‘SSMNet’) that are primarily located in high-risk urban areas of
 185 Switzerland, such as Basel and the Rhone Valley in the Valais (e.g., Clinton *et al.*, 2011; Cauzzi & Clinton, 2013).
 186 The SSMNet network is concluding a multiannual renewal project (2009 - 2023) which involved the renovation
 187 and significant expansion of the network, as well as the systematic site characterization of all newly instrumented
 188 sites (Michel *et al.*, 2014; Swiss Seismological Service (SED) at ETH Zurich (2015); Hobiger *et al.*, 2021). In
 189 addition to these permanent stations, the network holds another ~70 temporary stations, e.g., for the monitoring
 190 of geothermal exploration (Swiss Seismological Service (SED) at ETH Zurich, 2006²); aftershocks and seismic
 191 sequences (Swiss Seismological Service (SED) at ETH Zurich, 2005³), mass movements (Swiss Seismological

² <https://doi.org/10.12686/SED/NETWORKS/G2> last accessed July 2023

³ <http://networks.seismo.ethz.ch/networks/8d/>

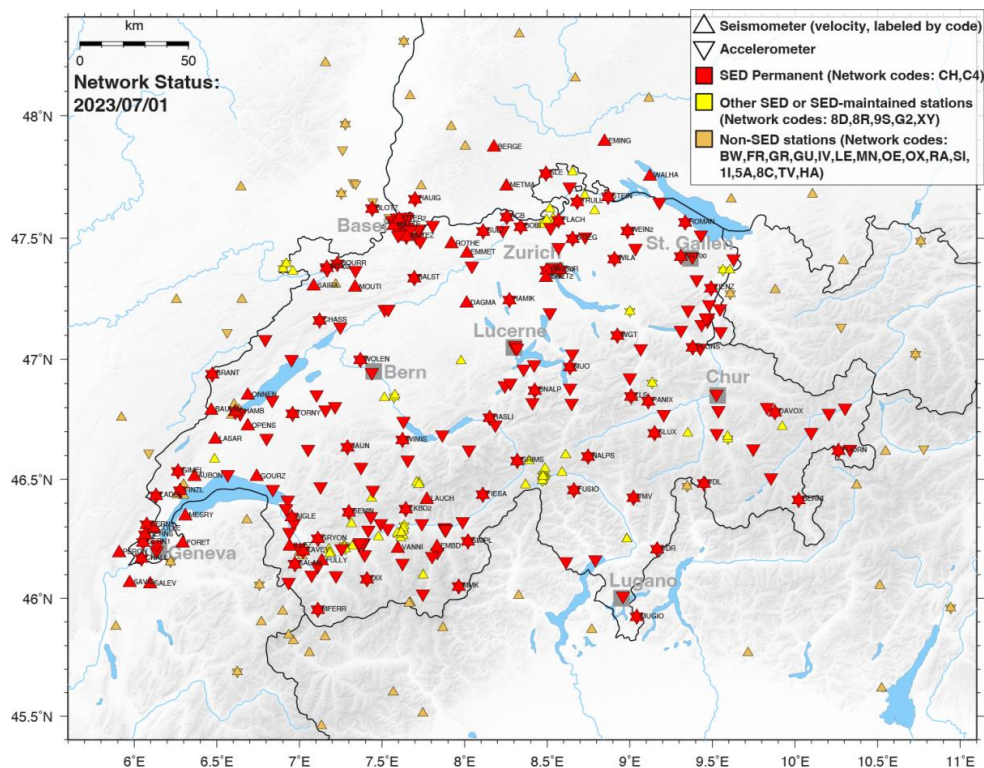


192 Service (SED) at ETH Zurich, 2012⁴), glaciers (Swiss Seismological Service (SED) at ETH Zurich, 1985⁵),
193 underground rock physics laboratories (Swiss Seismological Service (SED) at ETH Zurich, 2018⁶); as well as for
194 risk studies (Swiss Seismological Service (SED) at ETH Zurich, 2018⁷). The particularly dense network
195 infrastructure in the Valais is host to the Valais Near Fault Observatory (Chiaraluce et al., 2022). An extra ~10
196 stations inside Switzerland but operated by external providers are included in the SED processing to improve the
197 detection and characterization of seismic events, e.g., related to geothermal exploration (Swiss Seismological
198 Service (SED) at ETH Zurich, 2021⁸). Around 50 stations operated by seismic agencies in neighbouring countries
199 are included for regional real-time monitoring

200

201 In the Swiss network, the majority of broadband sensors are Streckeisen STS2 and STS2.5 and Nanometrics T240;
202 the Kinematics EpiSensor is deployed for strong-motion. The network uses modern ultra-low latency digitizers
203 (typically Nanometrics Centaur, Taurus, and Kinematics Q330), and most sensors are acquired at sampling rates
204 between 200 and 250 sps. A newly developed sensor concept allows the SED to easily deploy large numbers of
205 temporary stations rapidly in more remote locations with real-time streaming.

206



207

⁴ <https://doi.org/10.12686/SED/NETWORKS/XP>

⁵ <https://doi.org/10.12686/sed/networks/4d>

⁶ <https://doi.org/10.12686/SED/NETWORKS/8R>

⁷ <https://doi.org/10.12686/sed/networks/xy>

⁸ <https://doi.org/10.12686/sed/networks/5a>



208 **Figure 5: Map of Switzerland and the surrounding area showing broadband seismometers and strong-motion**
209 **accelerometers monitored by the Swiss Seismic Network as of July 2023. The map shows permanent and temporary**
210 **stations operated by the SED, as well as stations operated by external partners in and outside of Switzerland.**

211

212

213 **2.2 Seismic Data Processing**

214 Over the past 20 years, the number of stations within the Swiss Seismic Network has grown steadily. Data began
215 to be continuously archived in 1999, with the advent of the first broadband sensors. Today, continuous data is
216 standard and the network collects around 20GB of data every day; the total archive size is currently close to
217 100TB. The Swiss Seismic Network operates a European Integrated Data Archive (EIDA) node (Strollo *et al.*,
218 2021), and the majority of the waveform data, along with the SED earthquake catalogue, is open and accessible
219 via community-standard International Federation of Digital Seismograph Networks (FDSN) web services for data
220 access and download.

221

222 Since 2012, the Swiss Seismic Network has been utilising SeisComp⁹, a software developed by the German
223 Research Centre for Geosciences (GFZ) Potsdam and GemPa GmbH¹⁰, for earthquake monitoring and seismic
224 data processing. SeisComp supports real-time data acquisition, archival, and distribution, as well as automated
225 earthquake detection and quantification, manual earthquake review, as well as catalogue management.

226 **Detection and Location:** The real-time automated processing at the SED involves event triggering using station-
227 specific short term-average (STA)/long term-average (LTA) thresholds, refined post-picking using Baer (Baer &
228 Kradolfer, 1987) and AIC pickers, association of picks using *scautoloc* or *scanloc* (Grigoli *et al.*, 2018), and
229 location of events with *nonlinloc* (Lomax *et al.*, 2000) using Swiss-specific 1D and 3D velocity models. Several
230 projects have been initiated at the SED over the last decades to improve the existing velocity models at different
231 scales. A first 3D P-wave velocity model for Switzerland was developed by Husen *et al.* (2003), followed by a
232 regional 3D local earthquake tomography (LET) P-wave velocity model by Diehl *et al.* (2009). A refined Pg and
233 Sg LET model (parametrization 10x10x4 km) was computed by Diehl *et al.* (2021a). In their study, Diehl *et al.*
234 (2021a) demonstrated that a sub-kilometer accuracy of epicenters can be achieved in most parts of Switzerland
235 by using Pg and Sg phases in combination with an accurate 3D velocity model and the dense seismic network
236 operated by the SED. Especially in very densely instrumented parts of the network, in which the distance to the
237 closest observing station is smaller than 1.5 times the focal depth for most of the seismicity, the new velocity
238 model also achieves sub-kilometer accuracy of focal depths as demonstrated in Diehl *et al.* (2021a) and Lee *et al.*
239 (2023). This 3D velocity model has been used for relocation and high-resolution seismotectonic interpretations in
240 several recent studies (e.g., Lanza *et al.*, 2022; Diehl *et al.*, 2023) and, since June 2022, is the standard model for
241 bulletin locations by the SED. Furthermore, the LET model was locally improved in southwestern Switzerland by
242 application of a staggered-grid approach, resulting in a 5x5x3 km model parametrization for the region of the
243 Rhone-Simplon Fault Zone (Lee, 2023). The SED is working on an extension of these models to the entire crust,
244 a Swiss-wide 3D Qp and Qs attenuation model, and a new Alpine-wide 3D P-wave crustal model using the data
245 of the AlpArray experiment (e.g., Hetényi *et al.*, 2018).

⁹ <https://www.seiscomp.de/> last accessed July 2023

¹⁰ <https://www.gempa.de/> last accessed July 2023



246

247

248 **Source Characterization:** Over the last few years, the SED has updated its strategy for magnitude determination
249 to align it with the latest developments in engineering seismology and seismic hazard studies in Switzerland. This
250 includes the adoption of a new local magnitude relationship MLhc (Edwards *et al.*, 2015; Racine *et al.*, 2020) and
251 the seamless computation of the moment magnitude, Mw, based on spectral fitting, MwSpec (Edwards *et al.*,
252 2010). Station corrections for local magnitudes have been included, and these changes have been implemented
253 retrospectively for all events since January 1, 2009. Since November 2021, MLhc is the authoritative Swiss-
254 specific local magnitude used by the SED, and its computation has been integrated with SeisComP. Magnitudes
255 are provided for all origins, and the best origin is selected using a SED developed origin score that considers the
256 number of picks, pick residuals, and azimuthal gap. For earthquakes larger than M2.5, alerts are automatically
257 sent to federal and cantonal authorities (Section 4.2), a ShakeMap is created (Section 3.3), and the strong-motion
258 portal¹¹ is populated. Manual review is performed using the SeisComP *scolv* GUI. For large events with MLhc
259 >3.5, manual moment tensors are calculated using the *scmtv* GUI and published in the annual/bi-annual reports
260 of the SED (e.g., Diehl *et al.*, 2021b). The earthquake catalogue is curated through *scolv*. The SED is currently
261 working on strategies to disseminate and visualise its existing first-motion and moment-tensor catalogues for
262 public access.

263

264 **Advanced Processing:** In addition to the SeisComP standard modules mentioned above, the SED has developed
265 internally, or with support from GemPa, specific modules for advanced processing. These include

- 266 • *scwfparam* for providing engineering parameters and input to ShakeMap (Cauzzi *et al.*, 2016);
267 • *scenvelope*, *scvsmag*, and *scfinder* for EEW (Massin *et al.*, 2021);
268 • *scdetect* for earthquake detection using template matching (see below);
269 • *scrtDD* for real-time double difference relocation (see below).

270 *Earthquake Detection from Template Matching - scdetect:* Real-time earthquake detection is crucial for the
271 characterization of earthquake sequences. *Scdetect* is a highly configurable module for real-time earthquake
272 detection based on template matching using computationally efficient waveform cross-correlation (Armbruster *et*
273 *al.*, 2022; Mesimeri *et al.*, 2023). The workflow of *scdetect* is fully integrated with the SeisComP architecture and
274 allows users to visualize and refine the detected earthquakes using SeisComP's built-in GUI applications. *Scdetect*
275 is currently being real-time tested in Switzerland in areas of high seismic activity using templates from past
276 earthquake sequences with the goal of detecting small magnitude earthquakes that are missed by the current
277 operational pipelines.

278

279 *Real-time Double Difference Relocation - scrtDD:* To understand the spatio-temporal evolution of natural and
280 induced seismicity, it is essential to have real-time, high-precision hypocenter locations, allowing to determine
281 the geometry and extent of seismically active faults, as well as the volume affected by stimulation procedures.

¹¹ <http://strongmotionportal.seismo.ethz.ch/home/> last accessed July 2023



282 The spatio-temporal evolution of seismicity can also provide information about fluid-flow processes and hydraulic
283 properties, including the existence of possible hydraulic connections (e.g., Diehl *et al.*, 2017). Although relative
284 relocation procedures have been developed for decades (e.g., Console & Di Giovambattista, 1987; Waldhauser &
285 Ellsworth, 2000), they are rarely applied in routine, real-time processing. To address this, the SED has developed
286 the *scriDD* software module, which performs real-time and near-real-time double-difference relocations following
287 the procedures described in Waldhauser & Ellsworth (2000) and Waldhauser (2009) within the SeisComp
288 architecture. The module combines differential times derived from automatic and manual picks as well as
289 waveform cross-correlation with archived data from nearby past events (Scarabello *et al.*, 2020). The differential-
290 time data are subsequently inverted to compute the single-event, relative location of a newly detected earthquake
291 with respect to the double-difference background catalogue following the procedure of Waldhauser (2009). The
292 module also includes the possibility to generate or update a double-difference background catalogue using the
293 standard multi-event double-difference method of Waldhauser & Ellsworth (2000). To ensure that new events are
294 continuously included in the background catalogue and that real-time relocations remain accurate in areas of
295 sparse background seismicity, the SED has implemented both single-event and multi-event relocation procedures
296 in their operational monitoring system since 2021. Currently, the SED is developing and testing concepts for more
297 advanced visualisation and dissemination of SED's double-difference catalogues.

298

299 Other advanced methods which are currently being explored and evaluated at the SED, include

300

301 *Noise interferometry*: To monitor variations in mechanical and structural properties in the crust, the SED is
302 applying seismic noise interferometry techniques, which involve reconstructing approximative Green's functions,
303 typically referred to as cross-correlation functions, by correlating continuous ambient seismic noise records (e.g.,
304 Nakata *et al.*, 2019). From the cross-correlation functions, ballistic waves are used to image the subsurface (e.g.,
305 Obermann *et al.*, 2016; Molinari *et al.*, 2020) and coda waves are used for time-lapse imaging (e.g., Obermann *et al.*,
306 2013, 2014). Unlike earthquakes, seismic noise offers a constant source of signals that can be recorded
307 anywhere on Earth. The spatial resolution of noise interferometry is primarily limited by the geometry and
308 aperture of the seismic network, as well as the stability in noise excitation across frequency bands. While sparse,
309 noisy stations often only allow the reconstruction of the fundamental-mode surface wave, quiet stations in dense
310 arrays allow the reconstruction of body waves with a much-increased depth resolution. In addition to the
311 monitoring of natural processes, coda wave-based noise interferometry has great potential for the time-lapse
312 monitoring of local engineering applications, such as dams, hydraulic stimulations, or carbon storage. Changes in
313 seismic velocity and waveform similarity at geothermal project sites may help in the future to detect unexpected
314 reservoir dynamics earlier than the microseismic response alone (Obermann *et al.*, 2015; Hillers *et al.*, 2015;
315 Toledo *et al.*, 2022; Sánchez-Pastor *et al.*, 2019). The SED is currently testing this method in Iceland in
316 preparation for potential Carbon Capture and Storage sites in Switzerland.

317

318 *Fiber-optic deformation sensing*: During the past decade, fibre-optic sensing techniques, previously used mostly
319 for perimeter security and infrastructure monitoring applications, have emerged as a new seismic recording
320 paradigm. In particular, Distributed Acoustic Sensing (DAS) offers high spatial resolution at the metre scale, as
321 well as a frequency bandwidth from mHz to kHz (e.g., Lindsey *et al.*, 2020; Paitz *et al.*, 2021). Complementing



322 conventional seismometer recordings, DAS fills a niche in cases where kilometre-long fibre-optic cables can
323 either be co-used or easily deployed. The former includes fibre-optic sensing in densely populated cities (Ajo-
324 Franklin *et al.*, 2019, Spica *et al.*, 2020), under water (Spica *et al.*, 2022) or in avalanche-prone regions (Paitz *et*
325 *al.*, 2023) with the help of telecommunication fibres. This enables urban subsurface imaging with a lateral
326 resolution on the order of 10 m, and the detection of earthquakes and avalanches for monitoring and early warning
327 purposes. On volcanoes, glaciers and ice sheets, fibre-optic cables for sensing applications can often be deployed
328 with relative ease, thereby providing new opportunities for high-resolution studies of volcanic or glacial dynamics
329 (Walter *et al.*, 2020; Klaasen *et al.*, 2021; Jousset *et al.*, 2022). More recent developments in integrated fibre-optic
330 sensing overcome the limited interrogation distance of DAS, typically several tens of kilometres, at the expense
331 of reduced spatial resolution (Marra *et al.*, 2018; Bogris *et al.*, 2022). Applications of integrated sensing for
332 seismic imaging and earthquake characterization, especially in the oceans, are promising but still in their infancy.

333

334 *Machine learning:* Over the last couple of years, machine learning and deep learning techniques have started to
335 rapidly transform earthquake seismology (e.g., Mousavi & Beroza, 2022). Automated seismic processing methods
336 are nowadays capable of producing large data products of high quality that match or even exceed the reliability
337 and fidelity of human processing experts. The SED is actively pursuing research in deep learning-based
338 earthquake science, including event classification, seismicity monitoring methods, site-characterization, planetary
339 seismology, and seismicity forecasts (e.g., Marandò *et al.*, 2012; Hammer *et al.*, 2013; Meier *et al.*, 2019; Dahmen
340 *et al.*, 2022). This work involves implementing various machine learning models for seismic phase detection,
341 arrival time estimation, signal/noise classification, phase association, first motion polarity classification, and
342 others. The SED uses non-machine learning based methods as benchmarks to evaluate the effectiveness of the
343 new approaches. For all monitoring tasks, the SED plans to compare established and available models against
344 newly-trained models and models transfer-learned using Swiss data. A crucial aspect of these efforts will be the
345 testing of the machine learning methods at various scales of seismicity monitoring, including underground
346 laboratory experiments, geothermal reservoir scales, as well as national and regional monitoring scales.

347

348 **3. Products and Services**

349

350 **3.1. Operational Earthquake (Loss) Forecasting (OEF & OELF)**

351

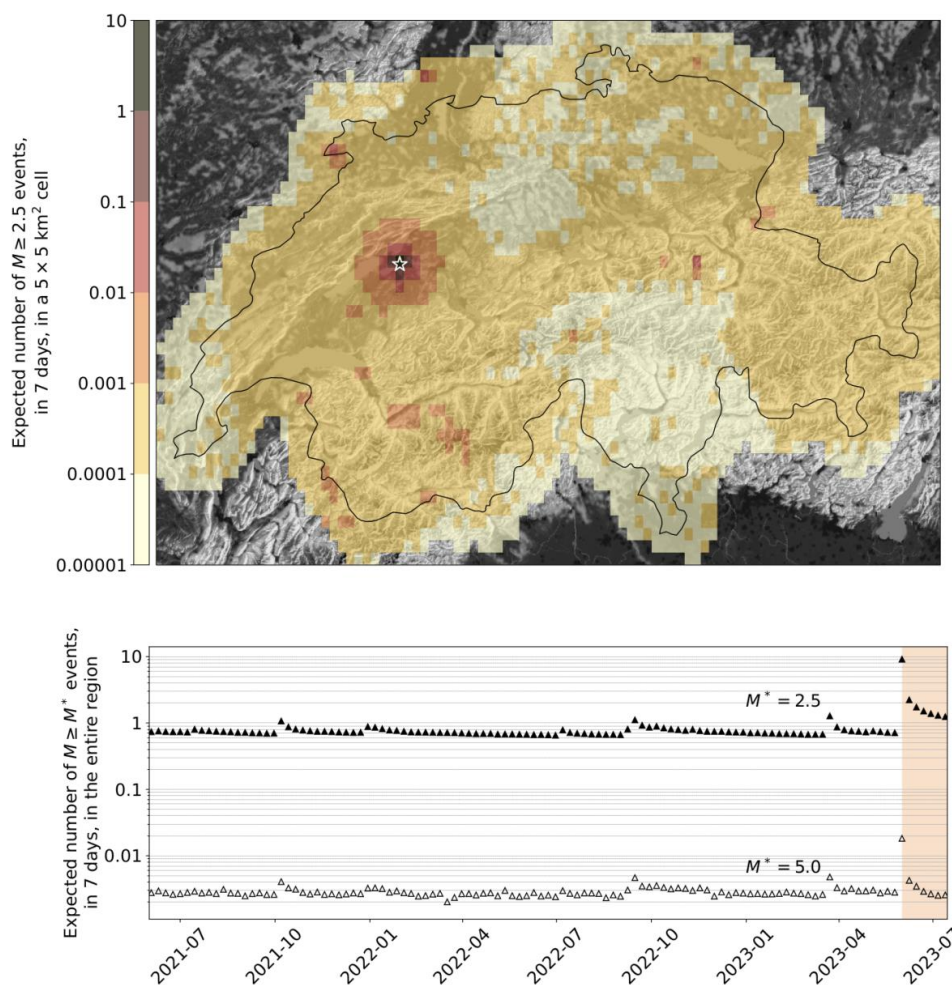
352 Operational Earthquake Forecasting (OEF) and Operational Earthquake Loss Forecasting (OELF) are scientific
353 approaches to forecasting the short-term probability of occurrence and the associated economic and societal
354 impact of earthquakes. OEF utilises statistical analysis of historical earthquake data, seismic activity patterns, and
355 geological features in a specific region to determine the probability of earthquakes above a certain magnitude
356 occurring over a given period. OELF builds upon these OEF probabilities and assesses the potential loss of life,
357 property, and infrastructure that could result.

358 Earthquake probabilities and the resulting short-term hazard and risk can vary by several orders of magnitude
359 between quiet periods and clustered sequences, such as aftershocks sequences or swarms (van Stiphout *et al.*,



360 2010). Unlike long-term earthquake forecasts, which inform long-term risk mitigation measures such as building
361 codes, the operationally calculated short-term earthquake probabilities and the corresponding loss estimates
362 generated by OEF and OELF, respectively, provide crucial information for crisis management in case of a major
363 magnitude event. To complement the long-term earthquake forecasts that are part of SUH2015, the SED is
364 therefore working on an Epidemic-Type Aftershock Sequence (ETAS)-based earthquake forecasting model for
365 Switzerland that describes the temporal fluctuations of earthquake probabilities. ETAS models (Ogata, 1988) are
366 widely used for OEF by agencies worldwide (Marzocchi *et al.*, 2014; Harte, 2019; van der Elst *et al.*, 2022) and
367 partition earthquakes into background seismicity and clusters of aftershocks. In the Swiss case, the background
368 seismicity model is based on the SUH2015 time-independent rate forecast, and clustered seismicity is modelled
369 using ETAS parameters calibrated with the local SED earthquake catalogue. The SED is developing and testing
370 multiple ETAS-based models for Switzerland (Mizrahi *et al.*, in prep.), ranging from simple models that only rely
371 on a comprehensive earthquake catalogue as input to more complex models that consider variations in catalogue
372 completeness and additional information from SUH2015. To evaluate the performance of the models, pseudo-
373 prospective forecasting experiments and retrospective consistency tests (Cattania *et al.*, 2018; Nandan *et al.*, 2021;
374 Bayliss *et al.*, 2022) are being conducted.

375 Besides the scientific model to probabilistically describe future earthquake occurrence, the SED is also developing
376 the IT infrastructure required to produce automated earthquake and loss forecasts for Switzerland in real-time (see
377 example in **Figure 6**). Both systems are initially operated internally at the SED for evaluation and refinement and
378 will at a later stage be made available to the general public and federal agencies in Switzerland. In particular, the
379 OELF system will provide actionable information to individuals, public authorities, and other stakeholders, based
380 on the updated earthquake rate forecast from the OEF system and ERM-CH23. Strategies for the effective
381 communication of earthquake probabilities and uncertainties to the public are important and have been and
382 continue to be extensively studied at the SED using surveys and discussions with focus groups and stakeholders
383 at the federal and cantonal levels (Section 4.2).



384

385 **Figure 6: Time-dependent earthquake forecast for Switzerland after a hypothetical Mw 6.0 earthquake near Bern,**
 386 **Switzerland, at midnight on June 1, 2023 (white star in top panel). Top: Spatial distribution of the expected number of**
 387 **felt earthquakes ($M_L \geq 2.5$) in the first 7 days following the event, per $0.05^\circ \times 0.05^\circ$ grid cell (roughly $5 \times 5 \text{ km}^2$).**
 388 **Temporal evolution of 7-day forecasts for the entire region shown in the top panel. The filled and empty triangles**
 389 **represent the expected number of $M_L \geq 2.5$ and $M_L \geq 5.0$ earthquakes, respectively. The shaded background marks**
 390 **the time interval after the occurrence of the Mw 6.0 event.**
 391

392 **3.2 Earthquake Early Warning (EEW)**

393

394 Earthquake early warning (EEW) systems are designed to rapidly detect earthquakes and provide people and
 395 automated systems with time to prepare and take protective action before strong shaking arrives (e.g., Allen *et al.*,
 396 2009; Cremen & Galasso, 2020). Although the EEW provided alert times are short (depending on the distance
 397 between the earthquake and the location to be warned), they are considered sufficient to allow taking cover,
 398 stopping trains or elevators, shutting down industrial processes, or triggering automated shutdown systems. EEW



399 is considered an important tool for earthquake risk reduction and disaster management, as it may help to reduce
400 the number of casualties and damage to infrastructure and buildings during an earthquake, as well as to minimise
401 social and economic disruption (e.g., Papadopoulos *et al.*, 2023).

402

403 For around one decade, the SED has been developing open-source software and methods for EEW using a set of
404 SeisComP modules (such as *scenvelope*, *scvsmag*, and *scfinder*), known as the ETHZ-SED SeisComP EEW (ESE)
405 system (Massin *et al.*, 2021). The core of ESE is formed by the Virtual Seismologist (VS; Cua, 2005) and Finite-
406 Fault Rupture Detector (FinDer; Böse *et al.*, 2012) algorithms. VS provides fast EEW magnitudes using existing
407 SeisComP detection and location modules, while FinDer identifies fault rupture extent by matching growing
408 patterns of observed high-frequency seismic acceleration amplitudes with modelled templates. The SED is
409 currently developing a new SeisComP module to compare the observed and predicted ground-motion envelopes
410 with the goal to select origins and magnitudes from the independent VS and FinDer source parameter estimates,
411 while suppressing false alerts (Jozinović *et al.*, *subm.*).

412 In Switzerland, VS and FinDer are not yet used for public alerting, but rather for testing and demonstration of
413 EEW. VS uses phase picks to provide fast locations and magnitudes for any event detected by the Swiss Seismic
414 Network, while FinDer is typically activated only for earthquakes with magnitudes greater than 3.5. The median
415 delay for the first VS (since 2014) and FinDer (since 2017) alert is 8.7 and 7 seconds, respectively, but earthquakes
416 are frequently detected in as little as 4 to 6 seconds when they occur in areas with a high station density (see
417 example in **Figure 7**). Typically, it takes 3.5 seconds for the P-waves to propagate from the hypocenter to the
418 fourth closest station in the Swiss Seismic Network. The SED continues to optimise the Swiss Seismic Network
419 for EEW, although the benefit from further station densification appears limited (Böse *et al.*, 2022). Despite the
420 rare occurrence of large earthquakes in Switzerland, a recent public survey shows that 70% of the Swiss population
421 would like rapid notifications for all earthquakes that are felt, even if they have a low damage potential (Dallo *et*
422 *al.*, 2022a). Future mass notifications for EEW in Switzerland could be enabled either through the Swiss multi-
423 hazard *Alertswiss* and *MeteoSwiss* platforms, which can receive and display push notifications on mobile devices,
424 or through cell broadcast once available.

425

426

427 **3.3 Swiss ShakeMaps**

428

429 Ground-motion maps provide critical information on the severity and distribution of ground shaking generated by
430 an earthquake. The SED has been utilising the ShakeMap® application (Worden *et al.*, 2020) in Switzerland for
431 approximately 15 years and is a core founder and contributor to the European ShakeMap initiative that promotes
432 international collaboration and harmonisation of ShakeMap procedures in the greater European region (Cauzzi *et*
433 *al.*, 2018b). ShakeMap rapidly maps seismic shaking information based on recorded and predicted intensity
434 measures, such as peak ground acceleration (PGA) and peak ground velocity (PGV), 5%-damped pseudo-
435 acceleration spectral ordinates (PSA), and macroseismic intensity levels, including amplification due to local site
436 effects.

437

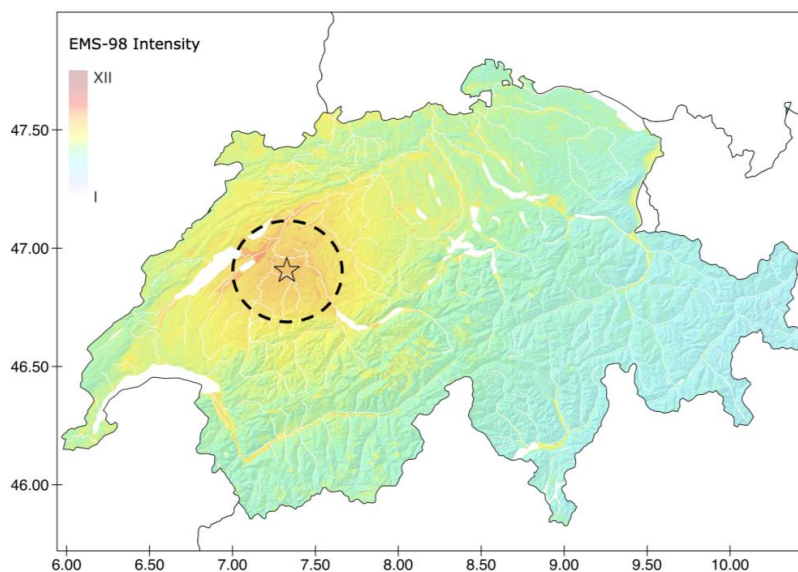


438 The SED ShakeMap framework is updated regularly and employs ground-motion models specific to Switzerland,
439 ground-motion-to-intensity conversion equations, and site amplification models (which are the same as those used
440 in ERM-CH23; Section 1.1) that allow for accurate and reliable ground shaking estimates across the Swiss alpine
441 and northern foreland regions (Cauzzi *et al.*, 2015). The SED maintains an archive of instrumental ShakeMaps
442 for events with a magnitude larger than 2.5 that occurred since 1991 and an atlas of large historical ShakeMaps
443 (see example in **Figure 7**). There are plans to include rapid finite-fault information in the SED ShakeMaps in the
444 near future (Böse *et al.*, 2012).

445

446 ShakeMaps are an important tool for earthquake response and recovery efforts. At the SED, ShakeMaps serve
447 multiple purposes. They are used (i) to inform the Swiss public about the severity of ground shaking and affected
448 areas; (ii) to estimate the likelihood of earthquake-triggered mass movements for significant events, following a
449 set of geospatial susceptibility proxies and peak ground acceleration (Cauzzi *et al.*, 2018); and (iii) to rapidly
450 assess the potential damage caused by ground shaking as part of the SED RIA system (Section 3.4).

451



452

453 **Figure 7: Swiss ShakeMap for a hypothetical Mw 6.0 earthquake near Bern. Dashed circle shows the 30-km-large no-**
454 **alert-zone centred on the epicentre where EEW could probably not be provided before strong shaking initiates.**

455

456

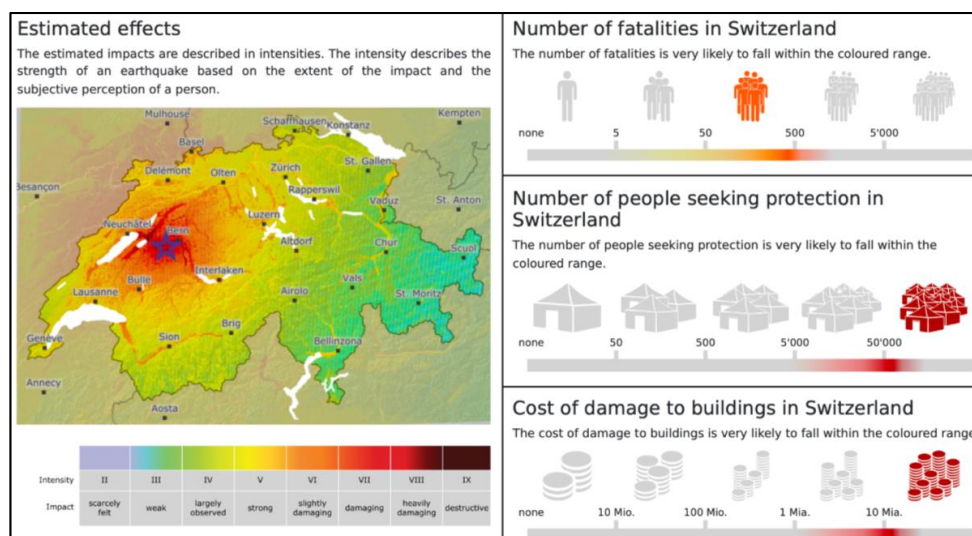
457 3.4 Rapid Impact Assessment (RIA)

458

459 Rapid Impact Assessment (RIA) involves the gathering and analysis of information to quickly assess the damage
460 and impact of an earthquake (or other) disaster. RIA systems shall provide decision-makers with timely and
461 accurate information to guide their response and recovery efforts. The RIA processing chain involves (i) the
462 assessment of the extent and severity of the damage; (ii) the evaluation of the needs of the affected population;
463 and (iii) the identification of priority areas for response. RIA efforts in Switzerland currently focus on the first
464 step.



465 The SED RIA system uses OpenQuake’s scenario calculator (Pagani *et al.*, 2014) and Swiss ShakeMaps (Section
 466 3.3). Once an earthquake’s location and magnitude are determined, a ShakeMap is created and the RIA calculator
 467 activated. Monte Carlo simulations are then used to generate multiple ground-motion field realisations at the
 468 location of the building assets in the ERM-CH23 exposure model. Damage and loss estimates are derived using
 469 the vulnerability functions associated with each asset and the simulated ground-motion values. The SED RIA
 470 system estimates various types of losses (damage, economic loss, injuries, deaths, and shelter needs) at the
 471 national, cantonal, and municipal levels. These estimates are compiled in a standard format (Section 4.2), which
 472 includes a map of ground shaking and visualisations of losses - along with associated uncertainties - at different
 473 scales. In the future, the SED RIA system will become fully integrated and synchronised with the Swiss Seismic
 474 Network operations and perform near-real-time calculations for every earthquake with magnitude $M > 3.0$ within
 475 a specified radius around Switzerland. For now, the RIA results (see example in **Figure 8**) are shared internally
 476 at the SED for verification, but will soon be made available to the public.



477
 478 **Figure 8: Exemplary Rapid Impact Assessment (RIA; @Swiss Seismological Service) output (here national level**
 479 **estimate) for a hypothetical Mw 6.0 earthquake near Bern. See [http://www.seismo.ethz.ch/static/ERM-](http://www.seismo.ethz.ch/static/ERM-CH23/scenario/Bern_M6_0_en.pdf)**
 480 **[CH23/scenario/Bern_M6_0_en.pdf](http://www.seismo.ethz.ch/static/ERM-CH23/scenario/Bern_M6_0_en.pdf) for full report.**

481

482 3.5 Seismic Hazard Web Platform and Services

483

484 Among other dynamic and operational earthquake-related services, the SED is actively involved in the
 485 development, maintenance, and hosting of a web platform that grants access to a wide range of earthquake hazard
 486 datasets, input models, results, documentation, and information at both the national and regional levels. This web
 487 platform, accessible at <http://hazard.efehr.org>, is an integral part of the European Facilities of the Earthquake
 488 Hazard and Risk (EFEHR) network of federated services. Moreover, the earthquake-related hazard data, products,



489 and services are designed to be interoperable with the newly developed EPOS ICS-C platform (Haslinger *et al.*,
490 2022).

491

492 The hazard platform comprises three individual web applications that enable users to interactively explore and
493 retrieve hazard curves, hazard spectra, and hazard maps. Through a user-friendly interface, users can access hazard
494 data and related metadata. The platform streamlines the retrieval of hazard maps, which can be disseminated to
495 users through multiple avenues, including customised services offering ASCII data, file downloads featuring
496 compressed ESRI shapefiles, and adherence to the OGC standards, which facilitate the distribution of projected
497 map images.

498

499 The EFEHR web portal serves as a gateway to various seismic hazard models, including the 1999 Global Hazard
500 Map of the Global Seismic Hazard Assessment Program (GSHAP, Giardini, 1999), the 2013 European Seismic
501 Hazard Model (ESHM13, Woessner *et al.*, 2015), the 2014 Earthquake Model of the Middle East (EMME14,
502 Giardini, 2017), the 2015 Swiss Hazard Model (SUIhaz15; Wiemer *et al.*, 2016), and the 2020 European Seismic
503 Hazard Model (ESHM20; Danciu *et al.*, 2021). Furthermore, this platform will be the principal repository for
504 results and datasets related to the ERM-CH23 (Wiemer *et al.*, 2023).

505

506

507 **3.6 Structural Health Monitoring (SHM)**

508

509 Due to slow retrofit and replacement rates of existing buildings, slow uptake of modern earthquake resistance
510 standards, and the intensity of extreme events, earthquakes pose a significant threat to the built environment. Post-
511 earthquake inspections are necessary to assess the damage to buildings and ensure safe shelter for the population.
512 Current expert-conducted visual inspections suffer from possible subjectivity and delay recovery. However, recent
513 advances in sensor development offer reliable and cost-effective sensing hardware, making broad monitoring of
514 multiple conventional buildings realistic. Structural Health Monitoring (SHM) provides tools to analyse these
515 sensor data and to translate vibration data into meaningful information about the structural state of a building.
516 Damage-sensitive features (DSFs) can be extracted from continuous measurements and contribute to the detection
517 and localization of earthquake-induced damage (e.g., Reuland *et al.*, 2023a).

518 Several approaches to overcome the scarcity of real-world dynamic monitoring data of both healthy and damaged
519 structures have been developed at the Chair of Structural Mechanics and Monitoring, ETH Zurich: (i) SHM-based
520 fragility functions relate probabilities of a structure to reach a given damage state to DSFs and can provide near-
521 real-time damage tags (Reuland *et al.*, 2021; Reuland *et al.*, 2023b); (ii) a machine-learning methodology relying
522 on domain adaptation has been successfully used to transfer a damage-state classification from simulated training
523 data to real measurements from experimentation (Martakis *et al.*, 2023); and (iii) a framework for automated
524 detection of faulty sensors has also been developed to ensure that sensors are functional and record valuable data
525 during earthquakes (Martakis *et al.*, 2022a). Furthermore, monitoring data from buildings can contribute to
526 earthquake preparedness by reducing uncertainty and regional variability of capacity curves used to derive
527 fragility functions (Martakis *et al.*, 2022b). After successful testing on individual buildings, SHM-based rapid loss



528 assessment has been recently integrated into a regional demonstrator (Nievas *et al.*, 2023). Integrating monitoring
529 data and engineering models into a robust framework will pave the way to make SHM-based real-time building
530 tagging operational in Switzerland and elsewhere.

531

532

533 **3.7 Recovery and Rebuilding Efforts (RRE)**

534

535 Recovery and Rebuilding Efforts (RRE) refer to the process of restoring a community or region to its pre-disaster
536 condition after a natural or man-made disaster. The recovery phase begins immediately after the event and focuses
537 on providing immediate assistance to affected people, restoring critical infrastructure such as power, water, and
538 transportation systems, and providing temporary housing for those displaced by the disaster. The rebuilding phase
539 involves longer-term efforts to repair or replace damaged infrastructure, such as roads, bridges, and buildings, and
540 to help affected individuals and communities recover from the economic and social impact of the disaster.

541

542 Resilient communities have the ability to quickly recover from extreme events, and retrofitting measures can help
543 decrease the risk of earthquakes and reduce repair efforts. Still, RRE is crucial to restoring community functions
544 and minimising negative social and economic impacts. Recovery models and resilience assessment tools can
545 simulate recovery trajectories and guide decision-makers towards effective actions. The iRe-CoDeS
546 (interdependent Resilience Compositional Demand and Supply) framework developed at ETH Zurich (Blagojević
547 *et al.*, 2022), offers the capacity to perform such analyses and has been integrated with OpenQuake software for
548 regional hazard and risk assessment.

549 Early loss assessment is often incomplete and imprecise, which hinders response efforts. To improve decision-
550 making, a dynamic update of regional post-earthquake damage estimates is proposed in iRe-CoDeS. Gaussian
551 Process inference models are used to fuse early inspection data with a pre-existing earthquake risk model (such
552 as ERM-CH23; Bodenmann *et al.*, 2023), reducing uncertainty and improving regional building damage
553 estimates. By combining regional recovery and resilience assessment tools with this framework, uncertainty in
554 recovery trajectories can be reduced, and real-time what-if analyses can inform decision-makers on the state of
555 the community during recovery and optimal resource deployment. The iRe-CoDeS model can be updated with
556 early inspection information after an earthquake, providing recommendations for recovery efforts and remaining
557 recovery time.

558

559

560 **4. Operation and Communication**

561

562 **4.1. Operation**

563

564 Providing operational services demands a high level of service availability. To achieve this, the SED provides
565 appropriate hardware solutions, invests in professional software engineering, and provides for 24/7 IT on-call
566 duty backup. The seismic processing data centre at the SED is the operational service with the longest history and



567 most mature setup, and provides the template for new services as they are added to the operational ecosystem.
568 High availability services are achieved by operating two identical software versions on fully redundant and
569 physically separated hardware, a primary and backup system. If any issues arise on the primary system, the backup
570 system can immediately become primary. A third server is also supported for development and prototyping.
571 Databases are also fully replicated and backed-up, and when database information is provided to the public, it is
572 accessed only via replicated databases to remove the possibility of external loads compromising the operational
573 systems.

574

575 To react to operational and seismic crises, the SED operates three 24/7 on-call teams, dedicated to technical IT-
576 related issues, immediate review of all seismic events with $M > 2.5$, and for handling inquiries from authorities,
577 media and the public for Swiss and international events. To provide internal and external seismic alerts, an in-
578 house developed alarm system enables the duty seismologists to take prompt action when an earthquake occurs.
579 The seismic alerts are automatically activated when an earthquake above a specific magnitude is detected within
580 or in proximity of Switzerland. Web portals enable the public distribution of products generated by these
581 operational services via direct access or APIs.

582

583 The SED conforms to international community standards in data formats, metadata and dissemination services
584 where possible (such as FDSN mseed, stationXML and web services), and indeed is at the cutting edge in
585 developing now standards, for example the SED curates the quakeML (Schorlemmer *et al.*, 2011) data model,
586 ensuring that earthquake information is easily accessible and shareable. The integration of harmonised data and
587 processes is at the heart of effective dynamic earthquake risk management and mitigation strategies.

588

589

590 **4.2 Communication and Societal Perspective**

591

592 As a federal agency, the SED is responsible for informing the public, authorities, and media about earthquakes in
593 Switzerland, and providing warnings when needed. For this purpose, the SED monitors ground shaking 24/7 in
594 Switzerland and neighbouring countries (Section 2.1). Details (including time, location, magnitude, and possible
595 impacts) of a detected earthquake are published on the SED webpage within 90 seconds. Federal and cantonal
596 authorities are informed automatically if the magnitude is 2.5 or larger. A team of on-call duty seismologists
597 assesses every recorded earthquake and takes further actions if needed, and is available for media requests. The
598 SED also engages in science communication during quiet times to transfer knowledge about earthquakes and
599 related topics. To ensure effective communication, the SED interacts with societal stakeholders and co-develops
600 and evaluates various information products, including those presented in this article. The SED also contributes to
601 the training of future earthquake experts through teaching efforts at ETH Zurich and beyond.

602 Recently, the SED has been shifting from hazard to risk communication, which should increase societies'
603 preparedness and disaster resilience. To ensure effectiveness, it is important that communication products are
604 designed by an interdisciplinary expert group and then tested with the relevant end-users before releasing them



605 publicly. In preparation of the ERM-CH23 release in March 2023, the SED has tested various output formats for
606 risk products with professional stakeholders of the society and the general public:

607 • Marti *et al.* (2023) showed that people and professionals consider RIA reports and risk scenarios to be
608 very important, although they appeared similarly challenged to correctly interpret the information
609 provided. To represent the uncertainties of the model estimates, the simplest visualisation using ranges
610 was the most understandable and the most popular (see **Figure 8**).

611

612 • Regarding EEW systems, a public survey conducted by the SED in Switzerland (Dallo *et al.*, 2022a),
613 revealed that the Swiss public wants to receive EEW alerts for all felt events (even if they are not
614 damaging) and their preferences align with those in other countries. EEW alerts with pictograms have
615 the strongest effect in motivating people to take action, even if that is not necessarily what they like best.

616

617 • The SED has collaborated with the Winton Center at the University of Cambridge to test OEF
618 communications with the general public in Italy, Switzerland, and California in the US. A survey of
619 Dryhurst *et al.* (2022) found that people in all three countries provided similar answers. Maps
620 representing OEF probabilities as different coloured isoline compartments could mislead the public. The
621 best information combination for OEF communication is a geographical map showing the forecast area,
622 textual information about the current absolute chance of an earthquake, and a risk ladder to provide
623 context.

624

625 • Dallo *et al.* (2022b) conducted three online surveys with various experiments and virtual focus groups
626 to improve communication of earthquake information on multi-hazard platforms, such as *MeteoSwiss*
627 and *Alertswiss* (Section 3.2). The results indicated that people prefer a combination of visual and textual
628 information, pictorial and textual behavioural recommendations, interactive features, consideration of
629 data privacy issues, messages with time indication and action-keywords, as well as clearly
630 distinguishable icons of the epicentre and the person's location (Valenzuela Rodríguez, 2021).

631

632 When designing information campaigns, it is important to consider people's personal factors, which can influence
633 their interpretation of the information provided, their design preferences, and their perceived usefulness. To
634 achieve successful campaigns, key factors to consider include regular communication, context, channel choice,
635 risk communicator training, and community-based approaches (Marti *et al.*, 2020). A significant challenge is to
636 provide personalised notifications to end-users while still addressing their concerns about data privacy.

637

638 **5. Conclusions and Outlook**

639

640 The SED is developing and implementing a harmonised and dynamic risk framework that centres around the
641 users' needs and considers earthquake hazard and risk as a constantly evolving, integrated concept. Significant
642 advancements in seismic observation in Switzerland were made over the past decade, including the



643 implementation of denser seismic networks and advanced data processing. They pave the path to enhance tools
 644 for earthquake forecasting, early warning, and rapid impact assessment and to harmonise them such that they are
 645 consistent, understandable and synergetic. We believe that by profiting from advances in scientific understanding
 646 and the dramatically changing technological capabilities, earthquake hazard and risk should be appreciated not as
 647 a constant in time, but as an evolving, integrated and dynamic risk (**Figure 1**).

648 According to our concept, the dynamic risk that a structure is exposed to depends on its structural type, location,
 649 occupancy, soil conditions, and topography, while people’s risk is affected by their exact location within a
 650 structure. However, dynamic risk also includes changes with time; for example, risk increases with rapid
 651 urbanisation and building stock changes or when a seismic sequence is active nearby, and can be observed by
 652 improved dynamic geophysical understanding of faulting and earthquake processes. EEW in the concept of
 653 dynamic risk is a sudden and short-term change in this risk environment (seconds to minutes); i.e. the time between
 654 rupture initiation and the arrival of damaging waves. RIA is likewise a defined state in dynamic risk: some
 655 buildings may be damaged by the preceding events thus changing their vulnerability in an environment of evolving
 656 seismic hazard because of an ongoing seismic sequence. Exposure of people has greatly changed, and the chance
 657 of another damaging earthquake is orders of magnitude higher than during a ‘normal’ day.

658 As data, models, and computing resources increase, dynamic and operational earthquake-related services will
 659 become increasingly available and important in assessing and mitigating earthquake risks. As described in
 660 previous sections, the SED provides key operational services, such as earthquake monitoring, ShakeMaps, EEW,
 661 OEF, RIA, and computational infrastructure. The seismic network and ShakeMap system are the most mature of
 662 these services, followed by EEW and RIA. The OEF service is currently in a demonstrator phase (**Table 1**).

663

664

665

Table 1: Status of earthquake risk-related products and services in Switzerland (as of July 2023).

Product/Service	Type	Status
Earthquake Hazard Model	product	available (SUIhaz2015)
Earthquake Risk Model	product	released (ERM-CH23)
Seismic Network	operational service	mature
Routine Seismic Data Processing	operational service	mature
ShakeMaps	operational service	mature (upgraded during RISE)
Earthquake Hazard Web-Services	operational service	mature
OE(L)F	demonstrator service	beta
EEW	demonstrator service	beta
RIA	demonstrator service	beta - operational



SHM	demonstrator service	beta
RRE	demonstrator software	available

666

667 Earthquake hazard and risk models are important for reducing the impact of earthquakes and increasing society's
668 resilience to disasters. The National Earthquake Risk Model of Switzerland (ERM-CH23, Wiemer *et al.*, 2023),
669 publicly released in March 2023, is expected to increase public awareness of earthquake risk and assist authorities
670 in updating their risk assessments and implementing mitigation measures. Further, it shall serve as a resource for
671 the insurance and reinsurance industry as well as the scientific community. Additionally, the ERM-CH23 serves
672 as the basis for other tools and systems being developed by the SED, such as RIA and OELF, which provide near-
673 real-time results and vital information after earthquakes.

674 To harmonise risk products and workflows, the SED is focusing on user needs and interoperability of the products
675 and services. The SED RIA system for Switzerland, for example, utilises the same ShakeMap provided in near-
676 real-time (Section 3.3), uses the same site amplification layers derived for the national risk models (Section 1.1),
677 and computes impact on people and buildings based on national databases of buildings and their vulnerability
678 (Section 3.4).

679 The SED is further advancing its seismic observational capabilities and risk products, including double-difference
680 earthquake catalogues, extending 3D crustal velocity models, enhancing magnitude determination, and exploring
681 new visualisation and distribution methods (Sections 2.1 & 2.2). They aim to offer short-term earthquake
682 probabilities and related seismic hazard and loss, provide rapid earthquake information and EEW to the Swiss
683 public, as well as integrate the RIA system into seismic network operations for near-real-time calculations for
684 earthquakes in and around Switzerland above magnitude 3.0.

685 The SED has a well-established communication network to provide rapid earthquake information over multiple
686 channels to the public (Section 4.2). Research is ongoing to determine how best to communicate earthquake
687 forecasts and support translation from probabilities into actions.

688

689 The SED has been investigating the use of a cost-benefit framework to evaluate earthquake dynamic risk products
690 such as OE(L)F, EEW, RLA, SHM, and RRE. While traditional Cost-Benefit Analysis (CBA) is effective for
691 evaluating EEW systems (e.g., Papadopoulos *et al.*, 2023) or OE(L)F based alerting systems (van Stiphout *et al.*,
692 2010; Hermann *et al.*, 2016), alternative methods such as Multi-Criteria Decision Analysis (MCDA) have proven
693 useful for decision-making when non-economic factors are significant (e.g., Guarini *et al.*, 2018). The flexibility
694 and transparency of MCDA allow for the consideration of a broader range of criteria beyond economic costs and
695 benefits, including model bias, model uncertainty, time gain in emergency response, information gain etc.,
696 therefore providing a valuable tool for assessing the cost-effectiveness of various dynamic risk products. Ongoing
697 research aims to evaluate the broader benefits of these dynamic risk products for earthquake risk reduction,
698 incorporating surveys and expert opinions to facilitate a dialogue with decision-makers and the public.

699



700 In a dynamic risk approach, the seismic activity is continually monitored by a regional seismic network, such as
701 operated by the SED, and risk assessments are adjusted in real-time based on the latest data. Compared to a static
702 risk approach which assumes a constant level of earthquake risk, the dynamic concept allows for more accurate
703 and timely identification of potential seismic hazards and risks. A dynamic risk approach is thus superior for a
704 seismic network because it provides a more accurate and up-to-date assessment of seismic risk, allowing for more
705 effective mitigation measures and improved safety outcomes.

706
707 In the dynamic risk framework (**Figure 3**) risk is assessed in a consistent and harmonised way for the next few
708 seconds or for the next five decades. This offers great potential for synergies, to achieve meaningful comparative
709 risk-cost-benefit analyses underpinned by a sustainable and quantitative framework that improves with time when
710 individual components improve. For example, in the near future, simulation-based approaches or so-called digital
711 twin components may replace certain elements of the framework, for example, physics-based ground motion
712 modelling. Adopting this conceptual framework of dynamic risk intrinsically implies a holistic and
713 interdisciplinary approach to earthquake risk assessment, risk reduction and resilience. It can also be extended in
714 a straightforward way to a multi-risk framework, providing significant added value to a range of challenges in
715 risk reduction.

716 **Acknowledgements**

717 This article was partially funded by the European Union's Horizon 2020 research and innovation program under
718 grant agreement No. 821115 "Real-time earthquake risk reduction for a reSilient Europe (RISE)"
719 (<http://www.rise-eu.org>). Opinions expressed in this paper solely reflect the authors' view; the EU is not
720 responsible for any use that may be made of the information it contains. The authors used OpenAI to improve
721 readability and language in some parts of the paper.

722

723

724 **Author contributions**

725 We use the [CRediT](#) Contributor Roles Taxonomy to categorise author contributions. **Methodology &**
726 **Investigation:** *Hazard and Risk:* LD, AP, PR, SW, PB, DF, FH, BMC, DG. *Seismic Monitoring (network &*
727 *processing):* JC, TD, CC, FM, FH, DF, AF, MB, FG, LH, PJ, DJ, FL, TL, M-AM, AO, MS, LS, AS, SW, PK.
728 *OE(L)F:* LM, SW, MH, LD, AP, PR. *EEW:* MB, FM, JC, DJ, CC. *ShakeMaps:* CC, JC, MB, PB, DF. *RIA:* LD,
729 AP, PR, NS, SW. *SHM:* YR, EC, LB, PM, BS, NB. *RRE:* YR, EC, LB, PM, BS, NB. **Communication:** ID, MM,
730 NV, LD, AP, PR. **Writing – original draft:** MB. **Writing – review & editing:** all. **Project investigators and**
731 **Funding:** DG, SW.

732 **Declaration of Competing Interests**

733 The authors acknowledge that there are no conflicts of interest recorded.

734



735 **References**

- 736 Ajo-Franklin, J., Dou, S., Lindsey, N., Monga, I., Tracy, C., Robertson, M., Rodriguez Tribaldos, V., Ulrich, C.,
737 Freifeld, B., Daley, T., and Li, X.: Distributed acoustic sensing using dark fiber for near-surface
738 characterisation and broadband seismic event detection, *Sci. Rep.*, 9, [https://doi.org/10.1038/s41598-018-](https://doi.org/10.1038/s41598-018-36675-8)
739 [36675-8](https://doi.org/10.1038/s41598-018-36675-8), 2019.
- 740 Al Atik, L., Abrahamson, N., Bommer, J. J., Scherbaum, F., Cotton, F., and Kuehn, N.: The Variability of Ground-
741 Motion Prediction Models and Its Components, *Seismological Research Letters*, 81, 794–801,
742 <https://doi.org/10.1785/gssrl.81.5.794>, 2010.
- 743 Allen, R. M., Gasparini, P., Kamigaichi, O., and Böse, M.: The status of earthquake early warning around the
744 world: an introductory overview, *Seism. Res. Lett.*, 80, 682–693, <https://doi.org/10.1785/gssrl.80.5.682>,
745 2009.
- 746 Armbruster, D., Mesimeri, M., Kaestli, P., Diehl, T., Massin, F., and Wiemer, S.: SCDetect: Near Real-Time
747 Computationally Efficient Waveform Cross-Correlation Based Earthquake Detection during Intense
748 Earthquake Sequences, *EGU GA*, <https://doi.org/10.5194/egusphere-egu22-12443>, 2022.
- 749 Bayliss, K., Naylor, M., Kamranzad, F., and Main, I.: Pseudo-prospective testing of 5-year earthquake forecasts
750 for California using inlabru, *Natural Hazards and Earth System Sciences*, 22 (10), 3231–3246, 2022.
- 751 Bear, M. and Kradolfer, U.: An automatic phase picker for local and teleseismic events, *Bull. Seismol Soc Am*,
752 77, 1437–1445, 1987.
- 753 Bergamo, P., Hammer, C., and Fäh, D.: Correspondence between Site Amplification and Topographical,
754 Geological Parameters: Collation of Data from Swiss and Japanese Stations, and Neural Networks-Based
755 Prediction of Local Response, *Bulletin of the Seismological Society of America*, 112(2), 1008–1030, 2021.
- 756 Bergamo, P. et al: A site amplification model for Switzerland based on site-condition indicators and incorporating
757 local response as measured at seismic stations, Submitted to *Bulletin of Earthquake Engineering*, 2023.
- 758 Blagojević, N., Hefti, F., Henken, J., Didier, M., and Stojadinović, B.: Quantifying disaster resilience of a
759 community with interdependent civil infrastructure systems, *Structure and Infrastructure Engineering*,
760 0(0), 1–15, <https://doi.org/10.1080/15732479.2022.2052912>, 2022.
- 761 Bodenmann, L., Reuland, Y., and Stojadinović, B.: Dynamic post-earthquake updating of regional damage
762 estimates using Gaussian processes, *Reliability Engineering & System Safety*, 234, 109201,
763 <https://doi.org/10.1016/j.ress.2023.109201>, 2023.
- 764 Bogris, A., Nikas, T., Simos, C., Simos, I., Lentas, K., Melis, N. S., Fichtner, A., Bowden, D., Smolinski, K.,
765 Mesaritakis, C., and Chochliourmos, I.: Sensitive seismic sensors based on microwave frequency fiber
766 interferometry in commercially deployed cables, *Sci. Rep.*, 12, [https://doi.org/10.1038/s41598-022-18130-](https://doi.org/10.1038/s41598-022-18130-x)
767 [x](https://doi.org/10.1038/s41598-022-18130-x), 2022.
- 768 Böse, M., Heaton, T. H., and Hauksson, E.: Real-time Finite Fault Rupture Detector (FinDer) for large
769 earthquakes, *Geophysical Journal International*, 191, 803–812, [https://doi.org/10.1111/j.1365-](https://doi.org/10.1111/j.1365-246X.2012.05657.x)
770 [246X.2012.05657.x](https://doi.org/10.1111/j.1365-246X.2012.05657.x), 2012.
- 771 Böse, M., Papadopoulos, A. N., Danciu, L., Clinton, J. F., and Wiemer, S.: Loss-Based Performance Assessment
772 and Seismic Network Optimization for Earthquake Early Warning, *Bulletin of the Seismological Society*
773 *of America*, 112, 1662–1677, <https://doi.org/10.1785/0120210298>, 2022.
- 774 Burjánek, J., Gischig, V., Moore, J. R., and Fäh, D.: Ambient vibration characterization and monitoring of a rock
775 slope close to collapse, *Geophysical Journal International*, 212(1), 297–310, 2018.
- 776 Cattania, C., Werner, M. J., Marzocchi, W., Hainzl, S., Rhoades, D., Gerstenberger, M., Liukis, M., Savran, W.,
777 Christophersen, A., and Helmstetter, A.: The forecasting skill of physics-based seismicity models during
778 the 2010–2012 Canterbury, New Zealand, earthquake sequence, *Seismological Research Letters*, 89(4),
779 1238–1250, 2018.
- 780 Cauzzi, C. and Clinton, J.: A High- and Low-Noise Model for High-Quality Strong-Motion Accelerometer
781 Stations, *Earthquake Spectra*, 29(1), 85–102, <https://doi.org/10.1193/1.4000107>, 2013.
- 782 Cauzzi, C., Edwards, B., Fäh, D., Clinton, J., Wiemer, S., Kästli, P., Cua, G., and Giardini, D.: New predictive
783 equations and site amplification estimates for the next-generation Swiss ShakeMaps, *Geophysical Journal*
784 *International*, 200(1), 421–438, <https://doi.org/10.1093/gji/egu404>, 2015.
- 785 Cauzzi, C., Behr, Y., Le Guenan, T., Douglas, J., Auclair, S., Woessner, J., Clinton, J., and Wiemer, S.: Earthquake
786 early warning and operational earthquake forecasting as real-time hazard information to mitigate seismic



- 787 risk at nuclear facilities, *Bulletin of Earthquake Engineering*, 14, 2495–2512,
788 <https://doi.org/10.1007/s10518-016-9864-0>, 2016a.
- 789 Cauzzi, C., Sleeman, R., Clinton, J., Ballesta, J. D., Galanis, O., and Kästli, P.: Introducing the European Rapid
790 Raw Strong-Motion Database, *Seismological Research Letters*, 87, 977–986,
791 <https://doi.org/10.1785/0220150271>, 2016b.
- 792 Cauzzi, C., Clinton, J., Faenza, L., Heimers, S., Koymans, M. R., Lauciani, V., Luzi, L., Michelini, A., Puglia,
793 R., and Russo, E.: Introducing a European integrated ShakeMap system, *Seismol. Res. Lett.*, 2018a.
- 794 Cauzzi, C., Fäh, D., Wald, D. J., Clinton, J., Losey, S., and Wiemer, S.: ShakeMap-based prediction of earthquake-
795 induced mass movements in Switzerland calibrated on historical observations, *Natural Hazards*, 92(2),
796 1211–1235, <https://doi.org/10.1007/s11069-018-3248-5>, 2018b.
- 797 Cauzzi, C. V., Clinton, J., Kaestli, P., Fäh, D., Bergamo, P., Böse, M., Haslinger, F., and Wiemer, S.: Swiss
798 Shakemap at Fifteen: Distinctive Local Features and International Outreach, in: *Seismological Society of
799 America Annual Meeting (SSA 2022)*, 2022.
- 800 Chiaraluca, L., Festa, G., Bernard, P., Caracausi, A., Carluccio, I., Clinton, J., Stefano, R., Elia, L., Evangelidis,
801 C., Ergintav, S., Jianu, O., Kaviris, G., Marmureanu, A., Sebela, S., and Sokos, E.: The Near Fault
802 Observatory community in Europe: a new resource for faulting and hazard studies, *Ann. Geophys.*, 65,
803 2022.
- 804 Console, R., and Di Giovambattista, R.: Local earthquake relative location by digital records. *Physics of the Earth
805 and Planetary Interiors*, 471, 43–49. [https://doi.org/10.1016/0031-9201\(87\)90065-3](https://doi.org/10.1016/0031-9201(87)90065-3), 1987.
- 806 Clinton, J., Cauzzi, C., Fäh, D., Michel, C., Zweifel, P., Olivieri, M., Cua, G., Haslinger, F., and Giardini, D.: The
807 current state of strong motion monitoring in Switzerland, *Earthquake Data in Engineering Seismology:
808 Predictive Models, Data Management and Networks*, 219–233, 2011.
- 809 Cremen, G. and Galasso, C.: Earthquake early warning: Recent advances and perspectives, *Earth-Science
810 Reviews*, 205, 103184, <https://doi.org/10.1016/j.earscirev.2020.103184>, 2020.
- 811 Crowley, H., Dabbeek, J., Despotaki, V., Rodrigues, D., Martins, L., Silva, V., Romão, X., Pereira, N., Weatherill,
812 G., and Danciu, L.: European seismic risk model (ESRM20), EFEHR Technical Report, 2,
813 <https://doi.org/10.3929/ethz-b-000590388>, 2021.
- 814 Cua, G. B.: Creating the Virtual Seismologist: Developments in Ground Motion Characterization and Seismic
815 Early Warning, Dissertation (Ph.D.), California Institute of Technology, [https://doi.org/10.7907/M926-
816 J956](https://doi.org/10.7907/M926-
816 J956) <https://resolver.caltech.edu/CaltechETD:etd-02092005-125601>, 2005.
- 817 Dahmen, N. L., Clinton, J. F., Meier, M. A., Stähler, S. C., Ceylan, S., Kim, D., Stott, A. E., and Giardini, D.:
818 MarsQuakeNet: A more complete marsquake catalog obtained by deep learning techniques, *Journal of
819 Geophysical Research: Planets*, 127(11), p.e2022JE007503, 2022.
- 820 Dallo, I., Marti, M., Clinton, J., Böse, M., Massin, F., and Zaugg, S.: Earthquake early warning in countries where
821 damaging earthquakes only occur every 50 to 150 years – The societal perspective, *International Journal
822 of Disaster Risk Reduction*, 83, 103, <https://doi.org/10.1016/j.ijdrr.2022.103441>, 2022a.
- 823 Dallo, I., Stauffacher, M., and Marti, M.: Actionable and understandable? Evidence-based recommendations for
824 the design of (multi-)hazard warning messages, *International Journal of Disaster Risk Reduction*, 74,
825 102917, <https://doi.org/10.1016/j.ijdrr.2022.102917>, 2022b.
- 826 Danciu, L., Nandan, S., Reyes, C., Basili, R., Weatherill, G., Beauval, C., Rovida, A., Vilanova, S., Sesetyan, K.,
827 Bard, P.-Y., Cotton, F., Wiemer, S., and Giardini, D.: The 2020 update of the European Seismic Hazard
828 Model: Model Overview, <https://doi.org/10.12686/a15>, 2021.
- 829 Danciu, L., Weatherill, G., Rovida, A., Basili, R., Bard, P.-Y., Beauval, C., Nandan, S., Pagani, M., Crowley, H.,
830 and Sesetyan, K.: The 2020 European seismic hazard model: milestones and lessons learned, in: *European
831 Conference on Earthquake Engineering and Seismology*, 3–25, 2022a.
- 832 Danciu, L. et al.: The 2020 European Seismic Hazard Model: Milestones and Lessons Learned, in: *Progresses in
833 European Earthquake Engineering and Seismology. ECEES 2022. Springer Proceedings in Earth and
834 Environmental Sciences*, Cham, https://doi.org/10.1007/978-3-031-15104-0_1, 2022b.
- 835 Diehl, T., Husen, S., Kissling, E., and Deichmann, N.: High-resolution 3-D P-wave model of the Alpine crust,
836 *Geophys. J. Int.*, 179(2), 1133–1147, <https://doi.org/10.1111/j.1365-246X.2009.04331.x>, 2009.
- 837 Diehl, T., Kraft, T., Kissling, E., and Wiemer, S.: The induced earthquake sequence related to the St. Gallen deep
838 geothermal project (Switzerland): Fault reactivation and fluid interactions imaged by microseismicity.



- 839 Journal of Geophysical Research: Solid Earth, 122(9), 7272–7290. <https://doi.org/10.1002/2017JB014473>,
840 2017.
- 841 Diehl, T., Kissling, E., Herwegh, M., and Schmid, S.: Improving Absolute Hypocenter Accuracy with 3-D Pg and
842 Sg Body-Wave Inversion Procedures and Application to Earthquakes in the Central Alps Region, *J.*
843 *Geophys. Res. Solid Earth*, 1–26, <https://doi.org/10.1029/2021jb022155>, 2021a.
- 844 Diehl, T., Clinton, J., Cauzzi, C., Kraft, T., Kaestli, P., Deichmann, N., Massin, F., Grigoli, F., Molinari, I., and
845 Böse, M.: Earthquakes in Switzerland and surrounding regions during 2017 and 2018, *Swiss J. Geosci.*,
846 106(3), 543–558, <https://doi.org/10.1007/s00015-013-0154-4>, 2021b.
- 847 Diehl, T., Madritsch, H., Schnellmann, M., Spillmann, T., Brockmann, E., & Wiemer, S.: Seismotectonic evidence
848 for present-day transtensional reactivation of the slowly deforming Hegau-Bodensee Graben in the
849 northern foreland of the Central Alps, *Tectonophysics*, 846, 229659, 2023.
- 850 Dryhurst, S., Mulder, F., Dallo, I., Kerr, J. R., McBride, S. K., Fallou, L., and Becker, J. S.: Fighting
851 misinformation in seismology: Expert opinion on earthquake facts vs. fiction, *Frontiers in Earth Science*,
852 10, <https://www.frontiersin.org/articles/10.3389/feart.2022.937055>, 2022.
- 853 Edwards, B., Allmann, B., Fäh, D., and Clinton, J.: Automatic computation of moment magnitudes for small
854 earthquakes and the scaling of local to moment magnitude, *Geophysical Journal International*, 183(1), 407–
855 420, <https://doi.org/10.1111/j.1365-246X.2010.04743.x>, 2010.
- 856 Edwards, B., Michel, C., Poggi, V., and Fäh, D.: Determination of Site Amplification from Regional Seismicity:
857 Application to the Swiss National Seismic Networks, *Seismological Research Letters*, 84, 611–621, 2013.
- 858 Edwards, B., Kraft, T., Cauzzi, C., Kastli, P., and Wiemer, S.: Seismic monitoring and analysis of deep geothermal
859 projects in St Gallen and Basel, Switzerland, *Geophysical Journal International*, 201, 1022–1039,
860 <https://doi.org/10.1093/gji/ggv059>, 2015.
- 861 ETH Zurich, S. S. S.: National Seismic Networks of Switzerland; ETH Zürich, Other/Seismic Network,
862 <https://doi.org/10.12686/SED/NETWORKS/CH>, 1983.
- 863 ETH Zurich, S. S. S.: The Site Characterization Database for Seismic Stations in Switzerland,
864 <https://doi.org/10.12686/sed-stationcharacterizationdb>, 2015.
- 865 Faenza, L. and Michelini, A.: Regression analysis of MCS intensity and ground motion parameters in Italy and
866 its application in ShakeMap, *Geophys. J. Int.*, 180, 1138–1152, 2010.
- 867 Faenza, L. and Michelini, A.: Regression analysis of MCS intensity and ground motion spectral accelerations
868 (SAs) in Italy, *Geophys. J. Int.*, 186, 1415–1430, 2011.
- 869 Fäh, D., and Huggenberger, P.: INTERREG III Projekt: Erdbebenmikrozonierung am südlichen Oberrhein.
870 Zusammenfassung, doi:10.3929/ethz-a-006412199, 2006.
- 871 Fäh, D., Giardini, D., Kästli, P., Deichmann, N., Gisler, M., Schwarz-Zanetti, G., Alvarez-Rubio, S., Sellami, S.,
872 Edwards, B., Allmann, B., Bethmann, F., Wössner, J., Gassner-Stamm, G., Fritsche, S., and Eberhard, D.:
873 ECOS-09 Earthquake Catalogue of Switzerland Release 2011 Report and Database, *Public catalogue*, 17,
874 4, 2011.
- 875 Fäh, D., Moore, J. R., Burjanek, J., Iosifescu, I., Dalguer, L., Dupray, F., Michel, C., Woessner, J., Villiger, A.,
876 and Laue, J.: Coupled seismogenic geohazards in Alpine regions., *Bollettino di geofisica teorica ed*
877 *applicata*, 53, 2012.
- 878 Fritsche, S., Fäh, D., and Schwarz-Zanetti, G.: Historical intensity VIII earthquakes along the Rhone valley
879 (Valais, Switzerland): primary and secondary effects, *Swiss Journal of Geosciences*, 105, 1–18, 2012.
- 880 Giardini, D., Wiemer, S., Fäh, D., and Deichmann, N.: Seismic hazard assessment of Switzerland, 2004.
881 *Publication Series of the Swiss Seismological Service*, ETH Zürich, 91 pages, 2004.
- 882 Giardini, D.: The global seismic hazard assessment program (GSHAP)—1992/1999, *Ann Geophys.*, 42(6), 1999.
- 883 Giardini, D., Danciu, L., Erdik, M., Sesetyan, K., Demircioglu, M., Akkar, S., Gülen, L., and Zare, M.: Seismic
884 Hazard Map of the Middle East, <https://doi.org/10.12686/a1>, 2017.
- 885 Glueer, F., Häusler, M., Gischig, V., and Fäh, D.: Coseismic Stability Assessment of a Damaged Underground
886 Ammunition Storage Chamber Through Ambient Vibration Recordings and Numerical Modelling,
887 *Frontiers in Earth Science*, 9, 773155, 2021.
- 888 Grigoli, F., Scarabello, L., Böse, M., Weber, B., Wiemer, S., Stefan, and Clinton, J. F.: Pick- and waveform-based
889 techniques for real-time detection of induced seismicity, *Geophysical Journal International*, 213(2), 868–
890 884, <https://doi.org/10.1093/gji/ggy019>, 2018.



- 891 Guarini, M. R., Battisti, F., and Chiovitti, A.: A Methodology for the Selection of Multi-Criteria Decision Analysis
892 Methods in Real Estate and Land Management Processes, Sustainability, 10, 507,
893 <https://doi.org/10.3390/su10020507>, 2018.
- 894 Hammer, C., Ohrnberger, M., and Fäh, D.: Classifying seismic waveforms from scratch: a case study in the alpine
895 environment, Geophysical Journal International, <https://doi.org/10.1093/gji/ggs036>, 2013.
- 896 Harte, D. S.: Evaluation of earthquake stochastic models based on their real-time forecasts: a case study of
897 Kaikoura 2016, Geophysical Journal International, 217(3), 1894–1914, 2019.
- 898 Haslinger, F., Basili, R., Bossu, R., Cauzzi, C., Cotton, F., Crowley, H., Custodio, S., Danciu, L., Locati, M.,
899 Michelini, A., Molinari, I., Ottemöller, L., and Parolai, S.: Coordinated and interoperable seismological
900 data and product services in Europe: the EPOS thematic core service for seismology, Annals of
901 Geophysics, 65(2), 213, <https://doi.org/10.4401/ag-8767>, 2022.
- 902 Häusler, M., Gischig, V., Thöny, R., Glueer, F., and Donat, F.: Monitoring the changing seismic site response of
903 a fast-moving rockslide (Brien/Brinzauls, Switzerland), Geophysical Journal International, 229, 299–310,
904 2022.
- 905 Hengl, T., Heuvelink, G. B. M., and Rossiter, D. G.: About regression-kriging: From equations to case studies,
906 Computers & Geosciences, 33(10), 1301–1315, 2007.
- 907 Hermann, M., Zechar, J. D., and Wiemer, S.: Communicating time-varying seismic risk during an earthquake
908 sequence, Seismological Research Letters, 87, 301–312, <https://doi.org/10.1785/0220150168>, 2016.
- 909 Hetényi, G., Molinari, I., Clinton, J., Bokelmann, G., Bondár, I., Crawford, W. C., Dessa, J.-X., Doubre, C.,
910 Friederich, W., and Fuchs, F.: The AlpArray seismic network: a large-scale European experiment to image
911 the Alpine Orogen, Surveys in Geophysics, 39, 1009–1033, doi:10.1007/s10712-018-9472-4, 2018.
- 912 Hillers, G., Husen, S., Obermann, A., Planès, T., Larose, E., and Campillo, M.: Noise-based monitoring and
913 imaging of aseismic transient deformation induced by the 2006 Basel reservoir stimulation, Geophysics,
914 80(4), KS51–KS68, 2015.
- 915 Hobiger, M., Bergamo, P., Imperatori, W., Panzera, F., Lontsi, A. M., Perron, V., C., M., J., B., and Fäh, D.: Site
916 Characterization of Swiss Strong-Motion Stations: The Benefit of Advanced Processing Algorithms,
917 Bulletin of the Seismological Society of America, 111(4), 1713–1739, 2021.
- 918 Husen, S., Kissling, E., Deichmann, N., Wiemer, S., Giardini, D., and Baer, M.: Probabilistic earthquake location
919 in complex three-dimensional velocity models: Application to Switzerland, Journal of Geophysical
920 Research-Solid Earth, 108(B2), 2003.
- 921 Janusz, P., Bonilla, L. F., and Fäh, D.: URBASIS Deliverable: A case study on non-linear soil response in urban
922 areas, <https://doi.org/10.3929/ethz-b-000575536>, 2022.
- 923 Jousset, P., Currenti, G., Schwarz, B., Chalarí, A., Tilmann, F., Reinsch, T., Zuccarello, L., Privitera, E., and
924 Krawczyk, C. M.: Fibre optic distributed acoustic sensing of volcanic events, Nature communications, 13,
925 1753, 2022.
- 926 Jozinović, D., Massin, F., Böse, M., and Clinton, J.: Combining earthquake early warning solutions from different
927 algorithms: application to Switzerland, SSA abstract, 2023.
- 928 Klaasen, S., Paitz, P., Lindner, N., Dettmer, J., and Fichtner, A.: Distributed Acoustic Sensing in volcano-glacial
929 environments — Mount Meager, British Columbia, J. Geophys. Res., 159,
930 <https://doi.org/10.1029/2021JB022358>, 2021.
- 931 Kleinbrod, U., Burjánek, J., and Fäh, D.: Ambient vibration classification of unstable rock slopes: A systematic
932 approach, Engineering Geology, 249, 198–217, 2019.
- 933 Kremer, K., Fabbri, S. C., Evers, F. M., Schweizer, N., and Wirth, S. B.: Traces of a prehistoric and potentially
934 tsunamigenic mass movement in the sediments of Lake Thun (Switzerland), Swiss journal of geosciences,
935 115, 1–20, 2022.
- 936 Lanza, F., Diehl, T., Deichmann, N., Kraft, T., Nussbaum, C., Schefer, S., and Wiemer, S.: The Saint-Ursanne
937 earthquakes of 2000 revisited: evidence for active shallow thrust-faulting in the Jura fold-and-thrust belt,
938 Swiss Journal of Geosciences, 115, 2, doi: 10.1186/s00015-021-00400-x, 2022.
- 939 Lee, T., Diehl, T., Kissling, E., and Wiemer, S.: New insights into the Rhône–Simplon fault system (Swiss Alps)
940 from a consistent earthquake catalogue covering 35 yr, Geophysical Journal International, 232(3), 1568–
941 1589, <https://doi.org/10.1093/gji/ggac407>, 2023.



- 942 Lee, T.: The transition between Western and Central Alps: New seismotectonic insights from high-resolution
943 earthquake catalogs and tomography, Ph.D. Thesis, ETH Zurich, Diss No.: 29073. doi: 10.3929/ethz-b-
944 000613262, 2023.
- 945 Lindsey, N., Rademacher, H., and Ajo-Franklin, J.: On the broadband instrument response of fiber-optic (DAS)
946 arrays, *J. Geophys. Res.*, 125, <https://doi.org/10.1029/2019JB018145>, 2020.
- 947 Lomax, A., Virieux, J., Volant, P., and Berge, C.: Probabilistic earthquake location in 3D and layered models:
948 Introduction of a Metropolis-Gibbs method and comparison with linear locations, in: *Advances in Seismic
949 Event Location*, Thurber, C.H and N. Rabinowitz (eds.), Kluwer, Amsterdam, 101-134, 2000.
- 950 Marañón, S., Reller, C., Loeliger, H.-A., and Fäh, D.: Seismic waves estimation and wave field decomposition:
951 Application to ambient vibrations, *Geophys. J. Int.*, 191, 175–188, 2012.
- 952 Marra, G., Clivati, C., Luckett, R., Tampellini, A., Kronjäger, J., Wright, L., Mura, A., Levi, F., Robinson, S.,
953 Xuereb, A., Baptie, B., and Calónico, D.: Ultrastable laser interferometry for earthquake detection with
954 terrestrial and submarine cables, *Science*, 361, 486–490, 2018.
- 955 Martakis, P., Movsessian, A., Reuland, Y., Pai, S. G., Quqa, S., Garcia Cava, D., Tcherniak, D., and Chatzi, E.:
956 A semi-supervised interpretable machine learning framework for sensor fault detection, *Smart Struct. Syst.*
957 *Int. J.*, 29, 251–266, 2022a.
- 958 Martakis, P., Movsessian, A., Reuland, Y., Pai, S. G., Quqa, S., Garcia Cava, D., Tcherniak, D., and Chatzi, E.:
959 A semi-supervised interpretable machine learning framework for sensor fault detection, *Smart Struct. Syst.*
960 *Int. J.*, 29, 251–266, 2022b.
- 961 Marti, M., Stauffacher, M., and Wiemer, S.: Anecdotal evidence is an insufficient basis for designing earthquake
962 preparedness campaigns, *Seismological Research Letters*, 91, 4, <https://doi.org/10.1785/0220200010>,
963 2020.
- 964 Marti, M., Dallo, I., Roth, P., Papadopoulos, A. N., and Zaugg, S.: Illustrating the impact of earthquakes:
965 Evidence-based and user-centered recommendations on how to design earthquake scenarios and rapid
966 impact assessments, *International Journal of Disaster Risk Reduction*, 103674,
967 <https://doi.org/10.1016/j.ijdr.2023.103674>, 2023.
- 968 Marzocchi, W., Lombardi, A. M., and Casarotti, E.: The establishment of an operational earthquake forecasting
969 system in Italy, *Seismological Research Letters*, 85(5), 961–969, 2014.
- 970 Massin, F., Clinton, J., and Böse, M.: Status of Earthquake Early Warning in Switzerland, *Front. Earth Sci.*, 9,
971 <https://doi.org/10.3389/feart.2021.707654>, 2021.
- 972 Meier, M.-A., Ross, Z. E., Ramachandran, A., Balakrishna, A., Nair, S., Kundzicz, P., Li, Z., Andrews, J.,
973 Hauksson, E., and Yue, Y.: Reliable real-time seismic signal/noise discrimination with machine learning,
974 *Journal of Geophysical Research: Solid Earth*, 124, 788–800, <https://doi.org/10.1029/2018JB016661>,
975 2019.
- 976 Mesimeri, M., Armbruster, D., Kaestli, P., Scarabello, L., Diehl, T., Clinton, J., and Wiemer, S.: SCDetect: Real-
977 time computationally efficient waveform cross-correlation based earthquake detection, To be submitted to
978 *SRL*, 2023.
- 979 Michel, C., Edwards, B., Poggi, V., Burjánek, J., and Fäh, D.: Assessment of Site Effects in Alpine Regions
980 through Systematic Site Characterization of Seismic Stations, *Bulletin of the Seismological Society of
981 America*, 104(6), 2809–2826, 2014.
- 982 Michel, C., Fäh, D., Edwards, B., and Cauzzi, C. V.: Site amplification at the city scale in Basel (Switzerland)
983 from geophysical site characterization and spectral modelling of recorded earthquakes, *Physics and
984 Chemistry of the Earth*, 98, 27–40, 2017.
- 985 Mitchell-Wallace, K., Jones, M., Hillier, J., and Foote, M.: Natural catastrophe risk management and modelling.
986 Natural catastrophe risk management and modelling: A practitioner's Guide, 1st ed., John Wiley & Sons,
987 Hoboken, NJ, <https://doi.org/10.1002/9781118906057>, 2017.
- 988 Mizrahi, L., Nandan, S., and Wiemer, S.: Developing and Testing ETAS-Based Earthquake Forecasting Models
989 for Switzerland, In preparation.
- 990 Molinari, I., Obermann, A., Kissling, E., Hetényi, G., Boschi, L., and AlpArray-Easi Working, G.: 3D crustal
991 structure of the Eastern Alpine region from ambient noise tomography, in: *Results in Geophysical
992 Sciences*, 1–4, <https://doi.org/10.1016/j.ringps.2020.100006>, 2020.



- 993 Mousavi, S. M. and Beroza, G. C.: Deep-learning seismology, *Science*, 377,
994 <https://doi.org/10.1126/science.abm4470>, 2022.
- 995 Nakata, N., Gualtieri, L., and Fichtner, A. (Eds.): *Seismic ambient noise*, Cambridge University Press, 2019.
- 996 Nandan, S., Kamer, Y., Ouillon, G., Hiemer, S., and Sornette, D.: Global models for short-term earthquake
997 forecasting and predictive skill assessment, *The European Physical Journal Special Topics*, 230, 425–449,
998 2021.
- 999 Nievas, C. et al.: RISE deliverable 6.1: Integration of RISE Innovations in the Fields of OELF, RLA and SHM,
1000 in prep., 2023.
- 1001 Obermann, A., Planès, T., Larose, E., and Campillo, M.: Imaging preeruptive and coeruptive structural and
1002 mechanical changes of a volcano with ambient seismic noise, *Journal of Geophysical Research: Solid*
1003 *Earth*, 118, 6285–6294, 2013.
- 1004 Obermann, A., Froment, B., Campillo, M., Larose, E., Planès, T., Valette, B., Chen, J. H., and Liu, Q. Y.: Seismic
1005 noise correlations to image structural and mechanical changes associated with the Mw 7.9 2008 Wenchuan
1006 earthquake, *Journal of Geophysical Research: Solid Earth*, 119, 3155–3168, 2014.
- 1007 Obermann Kraft, T., Larose, E., and Wiemer, S.: Potential of ambient seismic noise techniques to monitor the St,
1008 Gallen geothermal site (Switzerland). *Journal of Geophysical Research: Solid Earth*, 120, 4301–4316,
1009 2015.
- 1010 Obermann, A., Lupi, M., Mordret, A., Jakobsdóttir, S.S., Miller, S.A., 2016. 3D-ambient noise Rayleigh wave
1011 tomography of Snæfellsjökull volcano, Iceland. *J. Vol. Geotherm. Res.* 317, 42–52.
1012 <https://doi.org/10.1016/j.jvolgeores.2016.02.013>.
- 1013 Ogata, Y.: Statistical models for earthquake occurrences and residual analysis for point processes, *Journal of the*
1014 *American Statistical Association*, 83, 9–27, <https://doi.org/10.1080/01621459.1988.10478560v>, 1988.
- 1015 Pagani, M., Monelli, D., Weatherill, G., Danciu, L., Crowley, H., Silva, V., Henshaw, P., Butler, L., Nastasi, M.,
1016 and Panzeri, L.: OpenQuake engine: An open hazard (and risk) software for the global earthquake model,
1017 *Seismological Research Letters*, 85, 692–702, [10.1785/0220130087](https://doi.org/10.1785/0220130087), 2014.
- 1018 Paitz, P., Edme, P., Gräff, D., Walter, F., Doetsch, J., Chalari, A., Schmelzbach, C., and Fichtner, A.: Empirical
1019 investigations of the instrument response for distributed acoustic sensing (DAS) across 17 octaves, *Bulletin*
1020 *of the Seismological Society of America*, 111, 1–10, 2021.
- 1021 Paitz, P., Lindner, N., Edme, P., Huguenin, P., Hohl, M., Sovilla, B., Walter, F., and Fichtner, A.: Phenomenology
1022 of avalanche recordings from distributed acoustic sensing, *J. Geophys. Res.*, 128,
1023 <https://doi.org/10.1029/2022JF007011>, 2023.
- 1024 Panzera, F., Bergamo, P., and Fäh, D.: Canonical Correlation Analysis Based on Site-Response Proxies to Predict
1025 Site-Specific Amplification Functions in Switzerland. *Bulletin of the Seismological Society of America*
1026 111(4):1905–1920, 2021.
- 1027 Panzera, F., Alber, J., Imperatori, W., Bergamo, P., and Fäh D.: Reconstructing a 3D model from geophysical
1028 data for local amplification modelling: The study case of the upper Rhone valley, Switzerland. *Soil*
1029 *Dynamics and Earthquake Engineering* 155:107163, 2022.
- 1030 Papadopoulos, A. N., Böse, M., Danciu, L., Clinton, J., and Wiemer, S.: A framework to quantify the effectiveness
1031 of earthquake early warning in mitigating seismic risk, *Earthquake Spectra*, 39, 938–961,
1032 [10.1177/87552930231153424](https://doi.org/10.1177/87552930231153424), 2023.
- 1033 Papadopoulos, A. N., Roth, P., Danciu, L., Bergamo, P., Panzera, F., Fäh, D., Cauzzi, C., Duvernay, B.,
1034 Khodaverdian, A., P., L., O., O., Fagà, E., Bazzurro, P., Marti, M., Valenzuela, N., Dallo, I., Schmid, N.,
1035 Kästli, P., Haslinger, F., and Wiemer, S.: in: *The Earthquake Risk Model of Switzerland ERM-CH23*,
1036 submitted to *Nat. Hazards Earth Syst. Sci.*, subm.
- 1037 Perron, V., Bergamo, P., and Fäh D.: Site Amplification at High Spatial Resolution from Combined Ambient
1038 Noise and Earthquake Recordings in Sion, Switzerland. *Seismological Research Letters*, 93(4):2281–2298,
1039 2022.
- 1040 Poggi, V., Edward, B., and Fäh, D.: A comparative analysis of site-specific response spectral amplification
1041 models. *Physics and Chemistry of the Earth* 98, 16–26. <http://dx.doi.org/10.1016/j.pce.2016.09.001>, 2017.
- 1042 Racine, R., Cauzzi, C., Clinton, J. et al.: Updated determination of earthquake magnitudes at the Swiss
1043 Seismological Service, EGU2020-8273, 2020.



- 1044 Reuland, Y., Martakis, P., and Chatzi, E.: Damage-sensitive features for rapid damage assessment in a seismic
1045 context, in: Proc. of the International Conference on Structural Health Monitoring of Intelligent
1046 Infrastructure, 613–619, 2021.
- 1047 Reuland, Y., Martakis, P., and Chatzi, E.: A comparative study of damage-sensitive features for rapid data-driven
1048 seismic structural-health monitoring, Applied Sciences. Under Review, 2023a.
- 1049 Reuland, Y., Khodaverdian, A., Crowley, H., Nievas, H., Martakis, P., and Chatzi, E.: Monitoring-driven post-
1050 earthquake building damage tagging, in: 10th International Conference on Experimental Vibration
1051 Analysis for Civil Engineering Structures, Milano, Italy, 2023b.
- 1052 Roten, D., Fäh, D., and Bonilla, L. F.: Quantification of cyclic mobility parameters in liquefiable soils from
1053 inversion of vertical array records, Bulletin of the Seismological Society of America, 104, 3115–3138,
1054 2014.
- 1055 Sägesser, R. und Mayer-Rosa, D: Erdbebengefährdung in der Schweiz. Schweizerische Bauzeitung Heft 7, 1978.
- 1056 Sánchez-Pastor, P., Obermann, A., Schimmel, M., Weemstra, C., Verdel, A., and Jousset, P.: Short-and long-term
1057 variations in the Reykjanes geothermal reservoir from seismic noise interferometry, Geophysical Research
1058 Letters, 46, 5788–5798, doi:10.1029/2019GL082352, 2019.
- 1059 Scarabello, L., Diehl, T., Kästli, P., Clinton, J., and Wiemer, S.: Towards Real-Time Double-Difference
1060 Hypocenter Relocation of Natural and Induced Seismicity, in: EGU General Assembly Conference
1061 Abstracts, <https://doi.org/10.5194/egusphere-egu2020-13058>, 2020.
- 1062 Schorlemmer, D., Euchner, F., Kästli, P., Saul, J., and Group, Q. W.: QuakeML: status of the XML-based
1063 seismological data exchange format, Annals of Geophysics, 54, doi: 10.4401/ag-4874, 2011.
- 1064 Shynkarenko, A., Kremer, K., Stegmann, S., Bergamo, P., Lontsi, A. M., Roesner, A., Hammerschmidt, S., Kopf,
1065 A., and Fäh, D.: Geotechnical characterization and stability analysis of subaqueous slopes in Lake Lucerne
1066 (Switzerland), Natural Hazards, 113, 475–505, 2022.
- 1067 SIA 261: Norm 261, Einwirkungen auf Tragwerke. Schweizerischer Ingenieur- und Architektenverein (SIA),
1068 Zürich, 2020.
- 1069 Silva, V., Amo-Oduro, D., Calderon, A., Costa, C., Dabbeek, J., Despotaki, V., Martins, L., Pagani, M., Rao, A.,
1070 and Simionato, M.: Development of a global seismic risk model, Earthquake Spectra, 36, 372–394, 2020.
- 1071 Spica, Z., Perton, M., Martin, E., Beroza, G., and Biondi, B.: Urban seismic site characterization by fiber-optic
1072 seismology, J. Geophys. Res., 125, <https://doi.org/10.1029/2019JB018656>, 2020.
- 1073 Spica, Z. J., Castellanos, J. C., Viens, L., Nishida, K., Akuhara, T., Shinohara, M., and Yamada, T.: Subsurface
1074 imaging with ocean-bottom distributed acoustic sensing and water phases reverberations, Geophysical
1075 Research Letters, 49, e2021GL095287, 2022.
- 1076 Strollo, A., Cambaz, D., Clinton, J., Danecek, P., Evangelidis, C. P., Marmureanu, A., Ottemöller, L., Pedersen,
1077 H., Sleeman, R., and Stammer, K.: EIDA: The European integrated data archive and service infrastructure
1078 within ORFEUS, Seismological Society of America, 92, 1788–1795, 2021.
- 1079 Strupler, M., Hilbe, M., Kremer, K., Danciu, L., Anselmetti, F. S., Strasser, M., and Wiemer, S.: Subaqueous
1080 landslide-triggered tsunami hazard for Lake Zurich, Switzerland, Swiss journal of geosciences, 111, 353–
1081 371, 2018.
- 1082 Swiss Seismological Service (SED) at ETH Zurich (1983): National Seismic Networks of Switzerland; ETH
1083 Zürich. Other/Seismic Network. <https://doi.org/10.12686/SED/NETWORKS/CH> DataCite
1084 metadata:HTML JSON XML
- 1085 Swiss Seismological Service (SED) at ETH Zurich (2015). The Site Characterization Database for Seismic
1086 Stations in Switzerland. Zurich: Federal Institute of Technology. doi: 10.12686/sed-
1087 stationcharacterizationdb
- 1088 Toledo, T., Obermann, A., Verdel, A., Martins, J. E., Jousset, P., Mortensen, A. K., Erbas, K., and Krawczyk, C.
1089 M.: Ambient seismic noise monitoring and imaging at the Theistareykir geothermal field (Iceland), Journal
1090 of Volcanology and Geothermal Research, 429, 107590,10.1016/j.jvolgeores.2022.107590, 2022.
- 1091 Valenzuela Rodríguez, N.: Die aktuelle Erdbebensituation der Schweiz visualisieren—Eine Analyse der
1092 Erdbebenkarte der MeteoSchweiz-App hinsichtlich ihrer Verständlichkeit und ihres
1093 Verbesserungspotenzials, [Master Thesis, Zurich University of Applied Sciences (ZHAW)].
1094 <https://www.polybox.ethz.ch/index.php/s/vaBmjfUr0AgaVtS>, 2021.



- 1095 Van der Elst, N. J., Hardebeck, J. L., Michael, A. J., McBride, S. K., and Vanacore, E.: Prospective and
1096 retrospective evaluation of the US Geological Survey Public aftershock forecast for the 2019–2021
1097 Southwest Puerto Rico Earthquake and aftershocks, *Seismological Society of America*, 93, 620–640, 2022.
- 1098 Van Stiphout, T., Wiemer, S., and Marzocchi, W.: Are short-term evacuations warranted? Case of the 2009
1099 L’Aquila earthquake, *Geophys. Res. Lett.*, 37, 1–5, <https://doi.org/10.1029/2009GL042352>, 2010.
- 1100 Waldhauser, F. and Ellsworth, W.: A Double-Difference Earthquake Location Algorithm: Method and
1101 Application to the Northern Hayward Fault, California, *Bulletin of the Seismological Society of America*,
1102 90, 1353–1368, <https://doi.org/10.1785/0120000006>, 2000.
- 1103 Waldhauser, F.: Near-real-time double-difference event location using long-term seismic archives, with
1104 application to Northern California, *Bull. Seismol. Soc. Am.*, 99(5), 2736–2748, doi:10.1785/0120080294,
1105 2009.
- 1106 Walter, F., Gräff, D., Lindner, N., Paitz, P., Köpfl, M., Chmiel, M., and Fichtner, A.: Distributed Acoustic
1107 Sensing of microseismic sources and wave propagation in glaciated terrain, *Nat. Comm.*, 11,
1108 <https://doi.org/10.1038/s41467-020-15824>, 2020.
- 1109 Wiemer, S., Danciu, L., Edwards, B., et al.: Seismic Hazard Model 2015 for Switzerland (SUHaz2015),
1110 <https://doi.org/10.12686/a2>, 2016.
- 1111 Wiemer, S., Papadopoulos, A., Roth, P., Danciu, L., Bergamo, P., Fäh, D., Duvernay, B., Khodaverdian, A.,
1112 Lestuzzi, P., Odabaşı, Ö., Fagà, E., Bazzurro, P., Cauzzi, C., Hammer, C., Panzera, F., Perron, V., Marti,
1113 M., N., V., Dallo, I., Zaugg, S., Fulda, D., Kästli, P., Schmid, N., and Haslinger, F.: Earthquake Risk Model
1114 of Switzerland (ERM-CH23), Swiss Seismological Service, ETH Zurich, <https://doi.org/10.12686/a20>,
1115 2023.
- 1116 Woessner, J., Danciu, L., Giardini, D., Crowley, H., Cotton, F., Grünthal, G., Valensise, G., Arvidsson, R., Basili,
1117 R., Demircioglu, M. B., Hiemer, S., Meletti, C., Musson, R. W., Rovida, A., Sesetyan, K., and Stucchi,
1118 M.: The 2013 European Seismic Hazard Model: key components and results, *Bulletin of Earthquake
1119 Engineering*, 13(12), 3553–3596, <https://doi.org/10.1007/s10518-015-9795-1>, 2015.
- 1120 Worden, C. B., Thompson, E. M., Hearne, M., and Wald, D. J.: ShakeMap Manual Online: technical manual,
1121 user’s guide, and software guide, U. S. Geological Survey, <https://doi.org/10.5066/F7D21VPQ>, 2020.